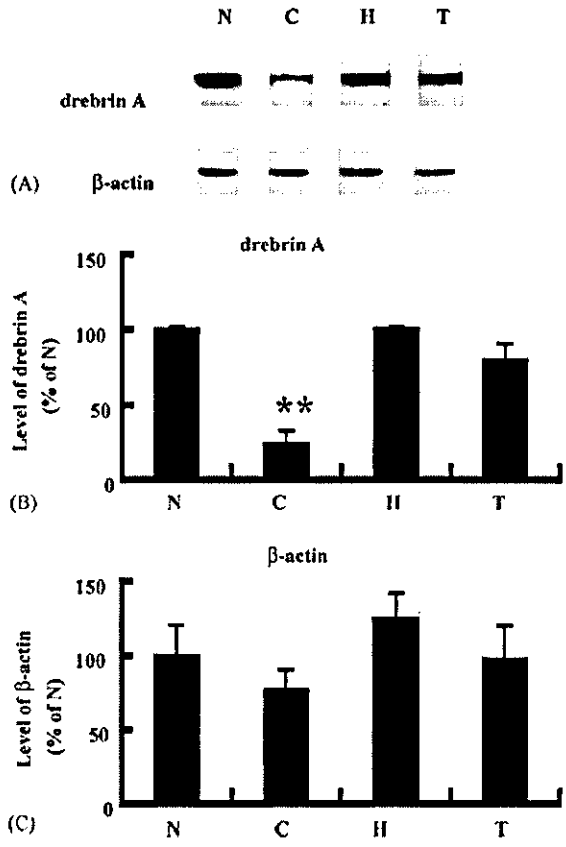

Fig. 1. Regional difference in the level of drebrin A protein expression in the brain of non-treated control rat. (A), Representative blots for drebrin A and β-actin obtained from the neocortex (N), cerebellum (C), hippocampus (H) and thalamus (T). Four μl of the homogenate (40 μg protein per lane) was loaded on 8% SDS gel for separation by electrophoresis. For measurement of β-actin as control protein, the membrane used for drebrin A was reprobed with monoclonal antibody against β-actin to confirm equal protein loading in each lane. (B–C) Quantitative analysis of relative band densities for drebrin A protein (B) and that for β-actin protein (C) obtained from the four brain structures. Level of drebrin A and β-actin protein in the four brain structures was represented as a percentage of that in the neocortex (N). Each value is an average of relative abundance of drebrin A protein or β-actin protein obtained from four non-treated rats ($n = 4$, mean ± S.E.M.). **Significantly different from the other three forebrain structures ($P < 0.01$).

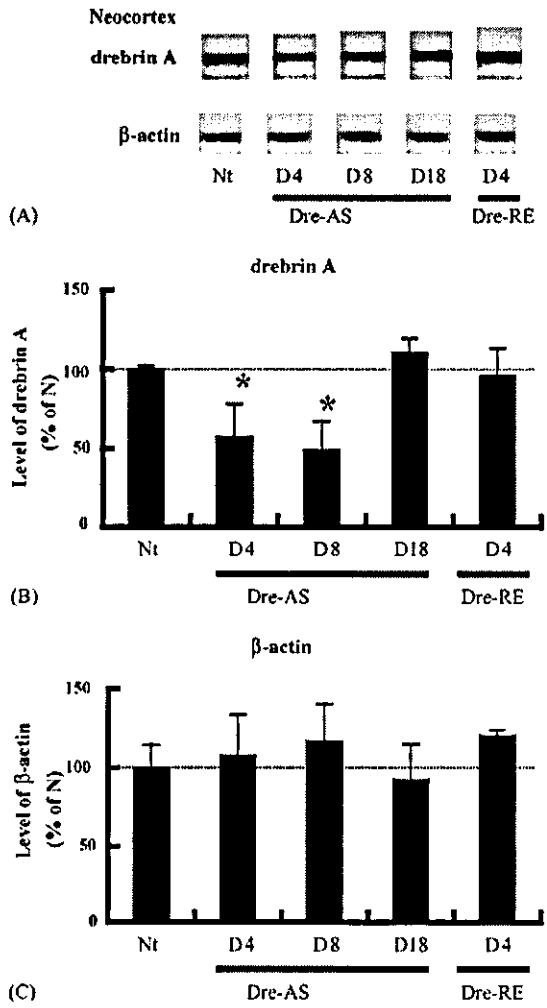

Fig. 2. Antisense-induced down-regulation of drebrin A protein expression in the neocortex and its time course following a single intra-ventricular injection of antisense ODNs to drebrin A by using HVJ-liposome mediated gene transfer method. Each treatment group: Nt, non-treated control rats; Dre-AS, rats that received an intra-ventricular injection of HVJ-liposome vectors containing antisense ODNs to drebrin A; Dre-RE, rats that received an intra-ventricular injection of HVJ-liposome vectors containing reversed antisense ODNs to drebrin A. (A) Representative blots for drebrin A and β-actin obtained from the neocortex of rats in each treatment group at 4 days (D4), 8 days (D8) or 18 days (D18) after an intra-ventricular injection of HVJ-liposome vectors containing ODNs. (B–C) Quantitative analysis of relative band densities for drebrin A protein (B) and β-actin protein (C) from the neocortex of rats in each treatment group. The relative density of each band was expressed as a percentage of the averaged density of bands in the Nt. Each value is an average of relative abundance of drebrin A or β-actin protein obtained from seven rats in each treatment group ($n = 7$, mean ± S.E.M.). *Significantly different from the Dre-RE (D4) ($P < 0.05$), and from the Nt and Dre-AS (D18) ($P < 0.01$).

injection, remained reduced for several days, and returned to the original level by 18 days post-injection, while the drebrin A protein levels in the Dre-RE-treated rats remained unchanged at 4 days post-injection. On the other hand, in the hippocampus of the Dre-AS-treated rats and Dre-RE-treated rats, the β-actin protein levels did not change at any time post-injection (Fig. 3A). As shown in the quantitative analysis for drebrin A protein levels (Fig. 3B), a significant reduction of 40.5 ± 8.9% (mean ± S.E.M., $n = 7$, 4 days post-injection) or 28.7 ± 11.8% (mean ± S.E.M., $n = 7$, 8 days post-injection) in drebrin A protein was specifically found in the hippocampus of the Dre-AS-treated rats and was sustained for more than a week, while the Dre-RE treatment did not affect the drebrin A protein levels. As shown in the quantitative analysis for β-actin protein levels (Fig. 3C), no significant change of the β-actin protein levels was found in the hippocampus of rats treated with Dre-AS or Dre-RE at any time post-injection.

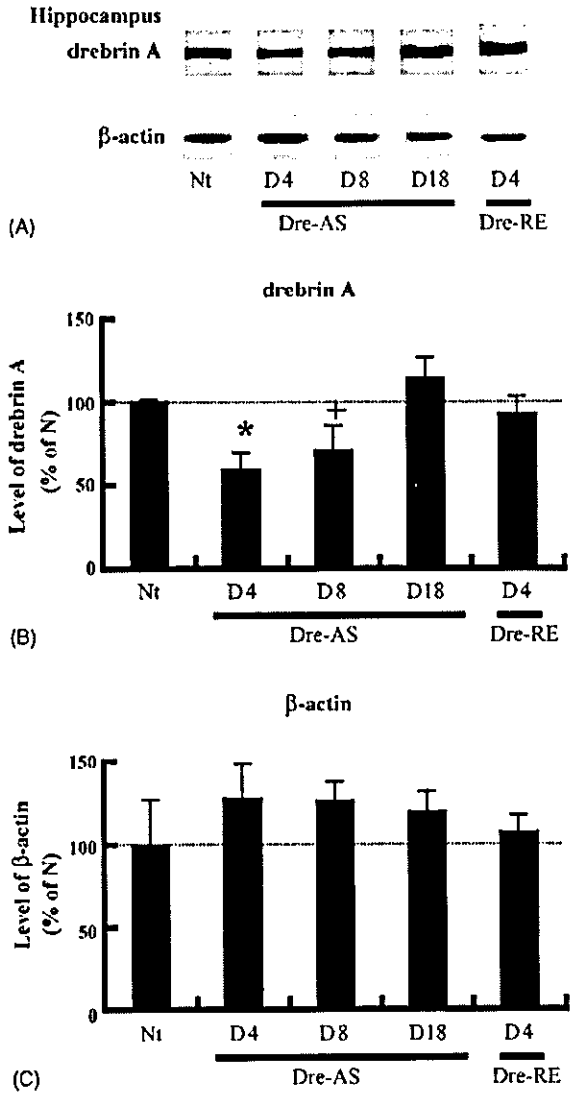

Fig. 3. Antisense-induced down-regulation of drebrin A protein expression in the hippocampus and its time course following a single intra-ventricular injection of antisense ODNs to drebrin A by using HVJ-liposome mediated gene transfer method. Each treatment group: Nt, non-treated control rats; Dre-AS, rats that received an intra-ventricular injection of HVJ-liposome vectors containing antisense ODNs to drebrin A; Dre-RE, rats that received an intra-ventricular injection of HVJ-liposome vectors containing reversed antisense ODNs to drebrin A. (A) Representative blots for drebrin A and β-actin obtained from the hippocampus of rats in each treatment group at 4 days (D4), 8 days (D8) or 18 days (D18) after an intra-ventricular injection of HVJ-liposome vectors containing ODNs. (B–C) Quantitative analysis of relative band densities for drebrin A protein (B) and β-actin protein (C) from the hippocampus of rats in each treatment group. The relative density of each band was expressed as a percentage of the averaged density of bands in the Nt. Each value is an average of relative abundance of drebrin A or β-actin protein obtained from seven rats in each treatment group ($n = 7$, mean ± S.E.M.). (+) Significantly different from the Nt ($P < 0.05$), and from the Dre-AS (D18) ($P < 0.01$). *Significantly different from the Dre-RE(D4) ($P < 0.05$), and from the Nt and Dre-AS (D18) ($P < 0.01$).

3.2. Increased spontaneous locomotion and abnormal adaptive behaviors in response to a novel environment in rats with drebrin A in vivo knockdown

To investigate the effects of antisense in vivo knockdown of drebrin A expression on adaptive behaviors in response to a novel environment, we recorded spontaneous locomotion and typical adaptive behaviors during a 30 min period in an open field test in rats that had received an intra-ventricular injection of HVJ-liposome vectors containing Dre-AS or Dre-RE 4 days prior to the open field test. The spontaneous locomotor activity was estimated by measuring the distance of locomotion during every 5 min period in the open field test of 30 min. On the other hand, the degree of typical adaptive behaviors, such as being exploratory, being stationary, or grooming in an open field, was estimated by measuring the total duration of being exploratory, being stationary, or grooming during the 30 min test period, respectively. The inserted figure in Fig. 4A shows the locomotor activity estimated by the total distance of spontaneous locomotion during the 30 min test period. As shown in the inserted figure, the locomotor activity in the Dre-AS-treated rats ($n = 9$) was significantly higher than that in the control Dre-RE-treated rats ($n = 6$). The time course of locomotor activity during the 30 min test period indicates that the significant increase of locomotor activity in the Dre-AS-treated rats is seen only in the earliest 5 min period during the 30 min open field test (Fig. 4A). As shown in Fig. 4B, the Dre-AS-treated rats ($n = 6$) were significantly less stationary and exhibited more grooming than the control Dre-RE-treated rats ($n = 5$).

3.3. Alterations in amphetamine-induced locomotor response in rats with drebrin A in vivo knockdown

To test whether abnormality of dopamine-related cortical functioning, which is believed to underlie some mental illnesses, is involved in behavioral alterations by the drebrin in vivo knockdown, we assessed the sensitivity to psychostimulant of the Dre-AS-treated rats using amphetamine-induced locomotor response. We measured locomotor activity in an open field during the 30 min period before amphetamine-injection (pre-injection phase) and the 60 min period after amphetamine-injection (post-injection phase) in rats that had received an intra-ventricular administration of HVJ-liposome vectors containing Dre-AS or Dre-RE 4 days prior to the amphetamine-induced locomotion test. The locomotor activity was estimated by measuring the locomotion during every 5 min period obtained from the total 90 min recording of locomotion in the open field. As shown in the post-injection phase in Fig. 5, a marked increase of the amphetamine-induced locomotor response was observed in the Dre-AS-treated rats. This increase by the Dre-AS treatment suggests that the Dre-AS-treated rats exhibit enhancement in the sensitivity to psychostimulant, compared with the sensitivity of the control Dre-RE-treated rats. It is notable that the degree of this increase of the

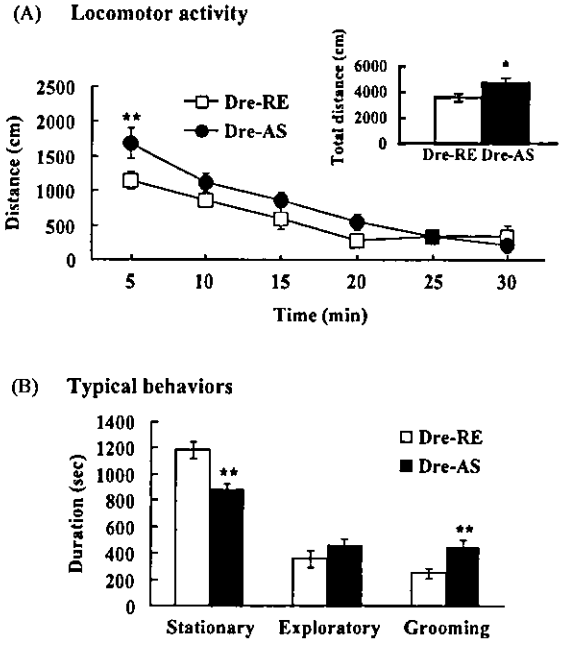

Fig. 4. Behavioral abnormalities in an open field test observed in rats with antisense in vivo knockdown of drebrin A expression. Treatment groups were: Dre-AS, rats that received a single intra-ventricular injection of HVJ-liposome vectors containing antisense ODNs to drebrin A 4 days prior to the open field test; Dre-RE, rats that received a single intra-ventricular injection of HVJ-liposome vectors containing reversed antisense ODNs to drebrinA 4 days prior to the open field test. The Dre-RE group was used as a control for the Dre-AS. (A) Increased locomotor activity in the Dre-AS rats during the open field test. Time-dependent change of spontaneous locomotor activity was estimated by locomotor distance during every 5 min following the start of locomotion in the open field. The inserted figure indicates the total locomotor distance during the 30 min test period. (B) Abnormal behavioral manifestations observed in the Dre-AS rats. Three typical behaviors that are characteristic of adaptive response to a novel environment: being stationary, being exploratory and grooming. Total duration of each behavioral manifestation was measured from the 30 min recording of behaviors in the open field by a chronometer, respectively. Each value represents mean ± S.E.M. ($n = 5$). *Significantly different from the Dre-RE ($P < 0.05$). **Significantly different from the Dre-RE ($P < 0.01$).

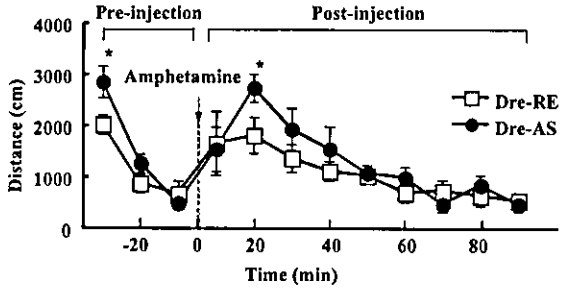

Fig. 5. Increased sensitivity to psychostimulant in an amphetamine-induced locomotor response observed in rats with antisense in vivo knockdown of drebrin A expression. Time-dependent change of locomotor activity before and after the intra-peritoneal injection of amphetamine was estimated by locomotor distance for every 5 min during the 30 min pre-injection and 60 min post-injection period. Treatment groups were: Dre-AS, rats that received a single intra-ventricular injection of HVJ-liposome vectors containing antisense ODNs to drebrin A 4 days prior to the amphetamine-induced locomotion test; Dre-RE, rats that received a single intra-ventricular injection of HVJ-liposome vectors containing reversed antisense ODNs to drebrinA 4 days prior to the amphetamine-induced locomotion test. The Dre-RE group was used as a control for the Dre-AS. Each value represents mean ± S.E.M. ($n = 6$). *Significantly different from the Dre-RE ($P < 0.05$).

amphetamine-induced locomotor response by the Dre-AS treatment and its recovery process are quite similar to that of the antisense-induced increase of the spontaneous locomotion in response to a novel environment, which is shown in the pre-injection phase in Fig. 5.

3.4. Reduction of pre-pulse inhibition and its recovery in rats with drebrin A in vivo knockdown

To examine whether the drebrin A in vivo knockdown causes a defect in the cognitive function, we used a PPI test of acoustic startle response. The PPI test was performed 4 and 18 days after the Dre-AS or Dre-RE treatment. The averaged startle amplitudes are shown in Table 1. The results from the PPI test performed 4 days after the treatment showed a significant disruption of PPI upon stimulation at PP70 but no significant disturbance of PPI at PP80 even

Table 1
Acoustic startle amplitudes in three types of stimulus trial and baseline amplitude in non-stimulus trial

Experiment	Treatment	Amplitudes in stimulus trial			
		B alone	P alone	PP70	PP80
Day 4	Dre-RE	5.2 ± 0.2	101.1 ± 15.1	40.5 ± 7.2	16.4 ± 1.7
	Dre-AS	4.7 ± 0.2	117.1 ± 20.9	71.0 ± 15.8	25.2 ± 4.9
Day 18	Dre-RE	5.0 ± 0.1	114.9 ± 23.9	46.2 ± 5.2	29.7 ± 7.2
	Dre-AS	6.3 ± 0.4	96.6 ± 4.2	45.0 ± 5.2	21.0 ± 1.5

Type of stimulus trial: B alone, non-stimulus trial to check the baseline amplitude without stimulation; P alone, stimulus trial with startle pulse alone; PP70, stimulus trial with the combination of startle pulse and 70 dB prepulse; PP80, stimulus trial with the combination of startle pulse and 80 dB prepulse. Experiment: Day 4, PPI test performed 4 days after the treatment with Dre-RE or Dre-AS; Day 18, PPI test performed 18 days after the treatment with Dre-RE or Dre-AS. Treatment group: Dre-RE, rats with intra-ventricular injection of reversed antisense ODNs to drebrin (Dre-RE); Dre-AS, rats with intra-ventricular injection of antisense ODNs to drebrin (Dre-AS). Each value represents mean ± S.E.M. ($n = 9$ for Day 4, $n = 6$ for Day 18).

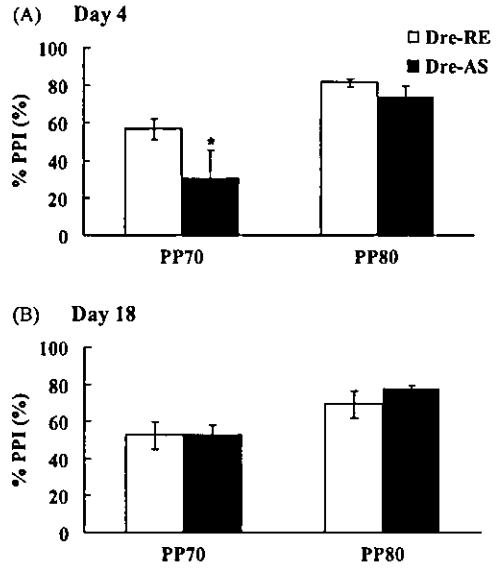

Fig. 6. Deficit of PPI of acoustic startle response and its recovery observed in rats with antisense in vivo knockdown of drebrin A expression. Treatment groups were: Dre-AS, rats that received a single intra-ventricular injection of HVJ-liposome vectors containing antisense ODNs to drebrin A 4 days or 18 days prior to the PPI test; Dre-RE, rats that received a single intra-ventricular injection of HVJ-liposome vectors containing reversed antisense ODNs to drebrinA 4 days or 18 days prior to the PPI test. The Dre-RE group was used as a control for the Dre-AS. The PPI was performed under two types of stimulation referred as PP70 and PP80. PP70 is an acoustic stimulation consisted of prepulse (20 ms burst of 70 dB) and startle-pulse (20 ms burst of 120 dB), while PP80 is that consisted of prepulse (20 ms burst of 80 dB) and startle-pulse (20 ms burst of 120 dB). (A) Percent prepulse inhibition in the Dre-AS or the Dre-RE 4 days after the ODNs-treatment. The rats treated with Dre-AS exhibited a significant disruption of PPI at the stimulation of PP70, but no disturbance of PPI at PP80 even though a slight tendency toward a reduced PPI. Each value represents mean ± S.E.M. ($n = 9$). *Significantly different from the Dre-RE ($P < 0.05$). (B) %PPI in the Dre-AS or the Dre-RE 18 days after the ODNs-treatment, when the down-regulated drebrin A expression has completely recovered to the original levels. The rats with Dre-AS treatment did not exhibit disruption of PPI at either PP70 or PP80, suggesting a recovery from the antisense-induced PPI deficit. Each value represents mean ± S.E.M. ($n = 6$).

though a slight tendency toward a reduced PPI was apparent compared with the control Dre-RE-treated rats (Fig. 6A). On the other hand, 18 days after the Dre-AS treatment, when the down-regulated drebrin A protein expression had completely recovered to the original levels, the Dre-AS-treated rats did not exhibit disruption of PPI at either PP70 or PP80 (Fig. 6B), suggesting a recovery from the antisense-induced PPI deficit.

3.5. Abnormality in the water-maze test in rats with drebrin A in vivo knockdown

To examine whether the antisense-induced down-regulation of drebrin A protein expression in the forebrain regions, such as the neocortex or hippocampus, causes an alteration in the acquisition of spatial reference memory, we used the Morris water-maze test. The rats received an intra-ventricular injection of HVJ-liposome vectors containing Dre-AS or Dre-RE 4 days prior to undergoing training in a water-maze. All of the rats in the treatment groups learned to swim directly to a hidden platform in five training sessions well before training was completed, as indicated in Fig. 7A. Compared with the rats treated with Dre-RE as a control group, a significant reduction in the escape latency was observed only in the earliest training session in the rats treated with Dre-AS.

On the last day of training, a spatial probe test was conducted just after the final training session. As shown in Fig. 7B, both Dre-AS-treated rats and control Dre-RE-treated rats spent more time in the target quadrant than in any other quadrant. However, surprisingly, the preference for the target quadrant observed in the Dre-AS-treated rats was significantly stronger than that in the control Dre-RE-treated rats, implicating that better spatial memory was acquired by the Dre-AS treatment.

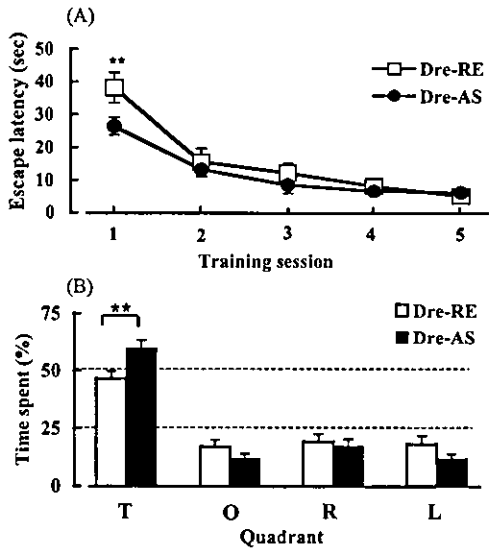

Fig. 7. Better memory in the hidden platform water-maze observed in rats with antisense in vivo knockdown of drebrin A. Treatment groups were: Dre-AS ($n = 9$), rats that received a single intra-ventricular injection of HVJ-liposome vectors containing antisense ODNs to drebrin A 4 days prior to the water-maze training; Dre-RE ($n = 6$), rats that received an intra-ventricular injection of HVJ-liposome vectors containing reversed antisense ODNs to drebrin A 4 days prior to the water-maze training. The Dre-RE group was used as a control for the Dre-AS. (A) Escape latency in water-maze training. Each value represents the averaged escape latency for 6 trials in each session (mean ± S.E.M.). The Dre-AS-treated rats displayed the greater learning ability during the first session in water-maze training than that of the Dre-RE. (B) Place preference in the spatial probe test conducted just after the end of training sessions. The Dre-AS-treated rats exhibited stronger preference for the target quadrant than that of the Dre-RE, suggesting that the Dre-AS-treated rats acquired better spatial memory. Quadrant was: T, target quadrant where the hidden platform was previously located; R, right quadrant; L, left quadrant; O, quadrant opposite to the target. **Significantly different from the Dre-RE ($P < 0.01$).

To clarify why the stronger preference for the target quadrant in Dre-AS-treated rats seems abnormal compared with that of non-treated control rats or Dre-RE-treated rats, we examined the time course of the place preference during 60 s probe trial. The upper panel of Fig. 8A shows a representative swimming track of a control Dre-RE-treated rat during the whole 60 s period of the probe test and its three divided tracks. The lower panel of Fig. 8A shows the place preference during every 20 s period following the start of the 60 s probe trial observed in control Dre-RE-treated

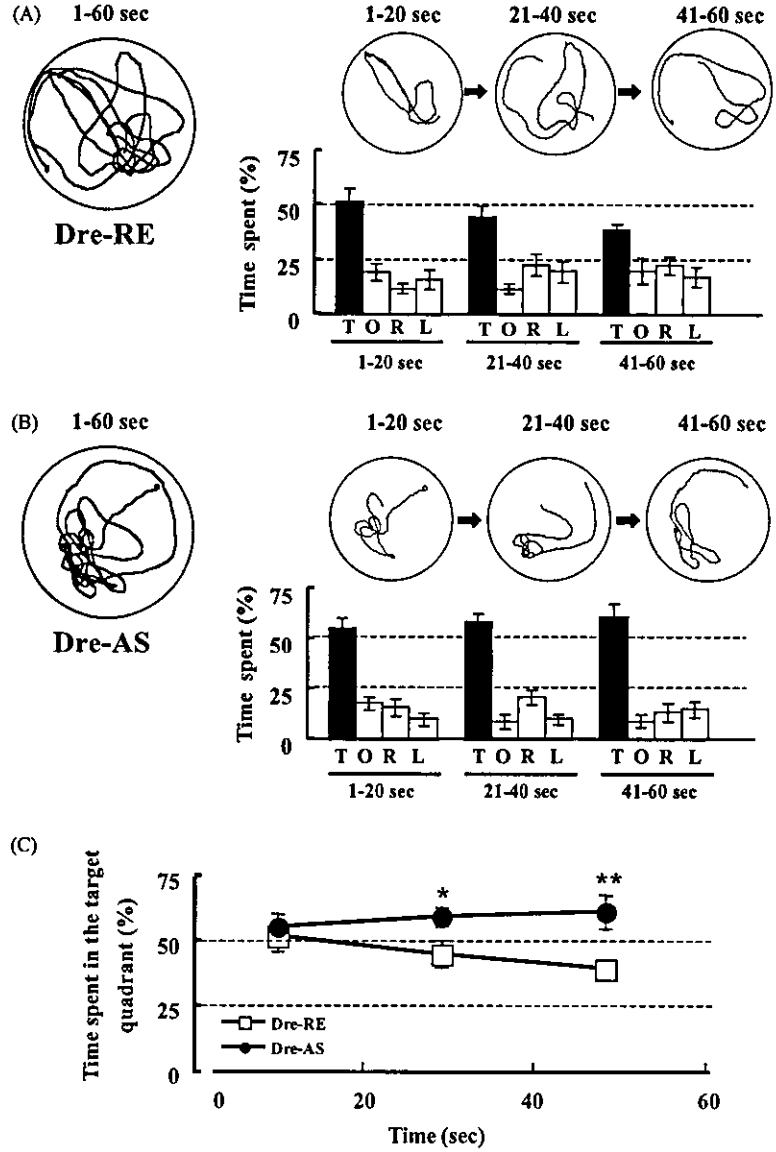

Fig. 8. Stronger preference for the target quadrant during the 60 s probe trial observed in rats with antisense in vivo knockdown of drebrin A. Treatment groups were: Dre-AS ($n = 9$), rats that received a single intra-ventricular injection of HVJ-liposome vectors containing antisense ODNs to drebrin A 4 days prior to the water-maze training; Dre-RE ($n = 6$), rats that received an intra-ventricular injection of HVJ-liposome vectors containing reversed antisense ODNs to drebrin A 4 days prior to the water-maze training. The Dre-RE group was used as a control for the Dre-AS. (A) Upper panel, representative swimming track of the control Dre-RE-treated rat during the 60 s period of the probe test and its three divided tracks; Lower panel, place preference during every 20 s period following the start of the 60 s probe trial observed in the Dre-RE-treated rats. The strong preference for the target quadrant in the Dre-RE rats declined within 60 s period of the probe trial. (B) Upper panel, representative swimming track of the Dre-AS-treated rat during the 60 s period of the probe test and those during every 20 s period following the start of a 60 s probe trial; Lower panel, place preference during every 20 s period following the start of the 60 s probe trial observed in the Dre-AS-treated rats. The strong preference for the target quadrant slightly increased within 60 s period of the probe trial. Unshadowed zone in the circle indicated the target quadrant, where the dense swimming track was depicted. (C) Time dependency of the strong preference for the target quadrant during 60 s period of the probe trial. In contrast to a decline in the strong preference for the target quadrant found in the Dre-RE-treated rats, the Dre-AS rats exhibited an abnormal persistence in the strong preference for the target quadrant. **Significantly different from the Dre-RE ($P < 0.01$). *Significantly different from the Dre-RE ($P < 0.05$).

rats ($n = 9$). As shown in the lower panel of Fig. 8A, the Dre-RE-treated rats as a control group exhibited a strong preference for the target quadrant zone in every 20 s period of the 60 s probe trial, but the level of preference for the target quadrant declined. This 60 s spatial probe test is originally designed to confirm an accomplishment of spatial learning by selection of a place preference in the water-maze without a hidden platform; that is, the same 60 s probe trial is not hypothesized to involve an additional behavioral response to the disappearance of the hidden platform task, which constitutes a problem that involves matching to sample. However, the decline in the preference for the target quadrant within the 60 s test period observed in the control rats suggests that behaviors in the 60 s spatial-probe test involve an adaptive response to a change of situation (namely, the disappearance of the hidden platform in the water-maze task), which is displayed by starting the searching behavior in quadrants other than the target quadrant in the water-maze. On the other hand, the upper panel of Fig. 8B shows a representative swimming track of the Dre-AS-treated rat during 60 s period of the probe test and its divided three tracks. The lower panel of Fig. 8B shows place preference during every 20 s period following the start of a 60 s probe observed in the Dre-AS-treated rats ($n = 9$). As shown in lower panel of Fig. 8B, the Dre-AS-treated rats exhibited a strong preference for the target quadrant in every 20 s period of the 60 s probe trial, and their preference for the target quadrant was sustained at the same level or slightly increased. As indicated in Fig. 8C, in contrast to the rapid decline that the control Dre-RE-treated rats exhibited in the preference for the target quadrant, the Dre-AS-treated rats displayed a rather slight increase in the level of their preference for the target quadrant within the 60 s probe trial. Thus, this abnormal persistence in the strong preference for the target quadrant zone in 60 s probe trial (Fig. 8C) suggests that the better spatial memory of the Dre-AS rats observed in Fig. 7B results from a cognitive deficit or worse judgment, which is revealed in their inability to inhibit inappropriate response to novel environment (namely, the disappearance of the hidden platform in the water-maze task).

4. Discussion

4.1. Antisense in vivo knockdown of drebrin A expression

We describe here the development of a rat with antisense-induced down-regulation of drebrin A protein levels in the drebrin-rich forebrain regions, such as the neocortex or hippocampus. The down-regulation of drebrin A protein levels that expressed 45–55% in the neocortex and 30–40% in the hippocampus was sustained for more than a week. The blocking effect of this intra-ventricular injection of antisense ODNs by using the HVJ-liposome method on the biosynthesis of drebrin A protein and the long-lasting action of antisense ODNs are equal to those of a repeated application or chronic infusion of antisense ODNs to NMDA-NR1 (Zapata et al., 1997). In a previous study, it was demonstrated that the Dre-AS we used here prevented the biosynthesis of drebrin A protein by about 48% in cultured cortical neurons (Takahashi et al., 2003; Tanaka et al., 2001). The present rate (45–55% in the cortex and 30–40% in the hippocampus) of an in vivo knockdown of drebrin A induced by the intra-ventricular administration of HVJ-liposome vectors containing Dre-AS was consistent with the rate of the in vitro knockdown of drebrin A induced by De-AS. In addition, since the transfection efficiency in vivo of HVJ-liposomes containing a plasmid DNA of constitutive nitric oxide synthase (c-NOS) has been reported to be 40–50% (Kaneda, 1999), the rate of an antisense in vivo knockdown of drebrin A by using HVJ-liposome vectors suggests that the biosynthesis of drebrin A in the transfected neurons is almost completely prevented by the long-lasting action of antisense ODNs, which are introduced into neurons bypassing the lysosomal attack. Thus, the degree of in vivo knockdown of drebrin A by a single intra-ventricular infusion of HVJ-liposome containing Dre-AS and its long-lasting action are sufficient to allow behavioral analysis for investigating the role of some specific proteins in higher brain functions without the stressful implantation of a cannula for repetitive or chronic administration.

4.2. Behavioral alterations induced by a drebrin A in vivo knockdown

Drebrin A in vivo knockdown rats display increased locomotor activity, a decreased stationary state, and enhanced grooming as adaptive behaviors in an open field and marked increase in an amphetamine-induced locomotor response (see Figs. 4 and 5). It could be considered that the decreased stationary state simply reflects the increase of locomotor activity due to unchanged locomotor velocity. Both increased locomotor activity in the earliest session and enhanced grooming in the open field test are a typical anxiety-like behavior for rodents as an adaptive response to a novel environment. It is commonly believed that changes in dopaminergic tone are highly related to alterations in locomotor activity (Amara and Kuhar, 1993; Giros et al., 1996), which explains the amphetamine-induced locomotor response. Therefore, the increase in amphetamine-induced locomotor response in the Dre-AS knockown rats, indicating their hypersensitivity, is thought to be an outcome of the increased sensitivity to psychostimulant in the drebrin knockdown rats. In addition to alteration in an emotional state, such as anxiety, alterations in locomotor behavior due to an increased sensitivity to psychostimulant have also been correlated with a positive symptom of schizophrenia (Corbett et al., 1995; Malhotra et al., 1997). Thus, an antisense-induced in vivo knockdown of drebrin A expression results in a number of altered behaviors that have been

traditionally characterized as modeling behaviors associated with schizophrenia. Indeed, mice treated with NMDA receptor antagonist PCP or MK-801, which have been regarded as animal models of schizophrenia, display an increase in both motor activity and sensitivity to psychostimulant (Abi-Saab et al., 1998; Duncan et al., 1999; Ellison, 1995; Javitt and Zukin, 1991; Malhotra et al., 1997).

In this study, we demonstrated that drebrin A knockdown rats display impaired PPI of the acoustic startle response at the stimulation type of PP70. Among a wide available range (65–85 dB) of pre-pulse intensity in acoustic stimulation, the pre-pulse intensity optimal to reveal the dysfunction of sensorimotor gating has been dependent on the types of treatment or disorder (Braff and Geyer, 1990; Braff et al., 2001; Inada et al., 2003). Thus, the present result indicates that the stimulation type of PP70 was more optimal than that of 80 dB for revealing PPI deficit in drebrin A knockdown rats. As shown in Fig. 6, the recovery from the deficit of PPI at PP70 in antisense-treated rats was observed at 18 days after the antisense treatment, when the down-regulated expression of drebrin A protein recovered to the original level. This recovery from the PPI deficit suggests that the disruption of PPI is dependent on the antisense-induced down-regulation of drebrin A in the forebrain such as the neocortex or hippocampus. It has been considered that the PPI reflects the function of the sensorimotor gating system, which partly overlaps with the cognitive function (Bakshi and Geyer, 1998; Braff and Geyer, 1990; Braff et al., 1992; Braff et al., 2001; Geyer, 1998), and that the disruption of PPI provides one of the modeling behaviors observed in schizophrenia, as schizophrenic patients display a significant impairment of PPI (Braff and Geyer, 1990; Braff et al., 1992; Braff et al., 2001; Geyer, 1998; Inada et al., 2003). Recently, it has been reported that an injection of non-competitive NMDA receptor antagonist into the dorsal hippocampus or amygdala produces the disruption of PPI in normal rats, suggesting that hypofunction of excitatory synapses in the multiple limbic regions mediates the PPI deficit (Bakshi and Geyer, 1998). Therefore, it is likely that the PPI deficit found in the drebrin in vivo knockdown rats results from dysfunction of excitatory synapses via antisense-induced modulation of dendritic spine function in the multiple limbic regions, such as the dorsal hippocampus or amygdala.

In the present study, global processes associated with spatial memory were impaired in drebrin A knockdown rats. In the spatial probe test, the preference for the target quadrant was stronger in the Dre-AS rats, suggesting that better memory was acquired by the Dre-AS treatment (see Fig. 7B). However, analysis of the perseverative behavior in the spatial probe test suggested that the stronger preference for the previous target in a novel environment observed in the Dre-AS rats (see Fig. 8) might rather result from a cognitive deficit or worse judgment than better memory, by which these rats are unable to inhibit inappropriate response or inattentive behavior to the sudden disappearance of the target. Another interpretation on the better spatial memory is that the abnormally strong preference for the previous target in the probe test may be due to a deficit in the naturally occurring extinction of memory. However, this interpretation is nearly the same as the cognitive deficit or worse judgment because the extinction of memory will occur when the animal is able to recognize being in any situation different from that memory event. Thus, the "better memory" observed in drebrin knockdown rats should be replaced by the term of "stronger preference" for previous experience due to cognitive deficit leading to perseverative tendencies. This behavioral abnormality in the water-maze resembles the cognitive dysmetria of the schizophrenic symptoms in the inability to receive and process information rapidly that has been associated with dysfunction of prefrontal–thalamic–cerebellar circuitry (Andreasen et al., 1996; Hecker et al., 1998; Wiser et al., 1998).

Because the swimming velocity of the Dre-AS rats in the first session was equal to that of the Dre-RE controls (data not shown), the reduced escape latency observed in the first session in the analysis of spatial memory formation seems to indicate that the drebrin A knockdown rats might have enhanced learning ability (see Fig. 7A). However, since the escape latency in the earliest training session depends largely on an animal's adaptive behaviors in a different situation from the previous event, this behavioral alteration may result from changes in the emotional or cognitive state rather than from increased learning ability. One possible interpretation of the shorter escape latency is also the stronger preference for the previous experience; that is, for the early trials when a maximum of 60 s swim time elapsed, rats were placed on the platform manually for 15 s, in an effort to force them to learn the hidden-platform task. Since most of the rats tested experienced this forced learning at least once, the stronger preference for the previous experience in the Dre-AS rats could make the escape latency shorter in the earlier session.

Due to the coincidence between several abnormal behaviors in drebrin in vivo knockdown rats and schizophrenia-related behaviors in rodents, there has been considerable interest in identifying the relationship between schizophrenic symptoms and dysfunction of excitatory synapses via antisense modulation of the drebrin–mediated dendritic spine function. The brain structures that have been correlated with the positive symptoms of schizophrenia, such as the prefrontal cortex, striatum, thalamus, dorsal hippocampus, or amygdala, largely overlap with the brain regions that have been characterized by high expression of dendritic spine protein drebrin A (see Fig. 1) (Hayashi et al., 1996) and the abundance of spiny neurons. Therefore, the combination of impaired adaptive behaviors, increased sensitivity to psychostimulant, and impaired PPI with stronger preference due to perseverative behavior observed in drebrin in vivo knockdown rats may provide a good animal model of schizophrenia. Further study is needed to demonstrate other schizophrenia-related behaviors, such as behavioral abnormalities in a forced-swim test or the negative symptoms of defective social interaction.

Acknowledgements

This study was supported by the Health Science Research Grants (no. H12-brain-018) from the Ministry of Health, Labor and Welfare, Japan. This investigation was also supported in part by the Grant for Scientific Research from Kitasato University Graduate School of Medical Science, Japan. We would like to thank Mr. Sakaguchi of Kitasato University for his kind help in the data analysis of water-maze test.

References

Abi-Saab, W.M., D'Souza, D.C., Moghaddam, B., Krystal, J.H., 1998. The NMDA antagonist model or schizophrenia: promise and pitfalls. Pharmacopsychiatry 31 (Suppl 2), 104–109.

Amara, S.G., Kuhar, M.J., 1993. Neurotransmitter transporters: recent progress. Annu. Rev. Neurosci. 16, 73–93.

Andreasen, N.C., O'Learly, D.S., Cizadlo, T., Arndt, S., Rezai, K., Ponto, L.L., Watkins, G.L., Hichwa, R.D., 1996. Schizophrenia and cognitive dysmetria: a positron-emission tomography study of dysfunctional prefrontal–thalamic–cerebellar circuitry. Proc. Natl. Acad. Sci. U.S.A. 93, 9985–9990.

Bakshi, V.P., Geyer, M.A., 1998. Multiple limbic regions mediate the disruption of prepulse inhibition produced in rats by the noncompetitive NMDA antagonist dizocilpine. J. Neurosci. 18, 8394–8401.

Braff, D.L., Geyer, M.A., 1990. Sensorimotor gating and schizophrenia: human and animal model studies. Arch. Gen. Psychiatry 47, 181–188.

Braff, D.L., Grillon, C., Geyer, M.A., 1992. Gating and habituation of the startle reflex in schizophrenic patients. Arch. Gen. Psychiatry 49, 206–215.

Braff, D.L., Geyer, M.A., Light, G.A., Sprock, J., Perry, W., Cadenhead, K.S., Swerdlow, N.R., 2001. Impact of prepulse characteristics on the detection of sensorimotor gating deficits in schizophrenia. Schizophr. Res. 49, 171–178.

Carlsson, M., Carlsson, A., 1990. Interaction between glutamatergic and monoaminergic systems within the basal ganglia: implications for schizophrenia and Parkinson's disease. Trends Neurosci. 13, 272–276.

Corbett, R., Camacho, F., Woods, A.T., Kerman, L.L., Fishkin, R.J., Brooks, K., Dunn, R.W., 1995. Antisychotic agents antagonize non-competitive *N*-methyl-D-aspartate antagonist-induced behaviors. Psychopharmacology (Berlin) 120, 67–74.

Duncan, G.E., Zorn, S., Lieberman, J.A., 1999. Mechanisms of typical and atypical antipsychotic drug action in relation to dopamine and NMDA receptor hypofunction hypotheses of schizophrenia. Mol. Psychiatry 4, 418–428.

Ellison, G., 1995. The *N*-methyl-D-aspartate antagonists phencyclidine, ketamine, dizoclipine as both behavioral and anatomical models of the dementias. Brain Res. Brain Res. Rev. 20, 250–267.

Engert, F., Bonhoeffer, T., 1999. Dendritic spine changes associated with hippocampal long-term synaptic plasticity. Nature 399, 66–70.

Geyer, M.A., 1998. Behavioral studies of hallucinohenic drugs in animals: implications for schizophrenia research, Pharmacopsychiatry Suppl. 2, 73–79.

Giros, B., Jaber, M., Jones, S.R., Wightman, R.M., Caron, M.G., 1996. Hyperlocomotion and indifference to cocaine and amphetamine in mice lacking the dopamine transporter. Nature 379, 606–612.

Harigaya, Y., Shoji, M., Shirao, T., Hirai, S., 1996. Disappearance of actin-binding protein drebrin, from hippocampal synapses in Alzheimer's disease. J. Neurosci. Res. 43, 87–92.

Hatanpaa, K., Isaacs, K.R., Shirao, T., Brady, D.R., Rapoport, S.I., 1999. Loss of proteins regulating synaptic plasticity in normal aging of the human brain and in Alzheimer disease. J. Neuropathol. Exp. Neurol. 58, 637–643.

Hayashi, K., Ishikawa, R., Ye, L.H., Takata, K., Kohama, K., Shirao, T., 1996. Modulatory role of drebrin in the cytoskeleton within dendritic spines in the rat cerebral cortex. J. Neurosci. 16, 7161–7170.

Hayashi, K., Shirao, T., 1999. Change in the shape of dendritic spines caused by overexpression of drebrin in cultured cortical neurons. J. Neurosci. 19, 3918–3925.

Hecker, S., Rauch, S.L., Goff, D., Savage, C.R., Schacter, D.L., Fischman, A.J., Alpert, N.M., 1998. Impaired recruitment of the hippocampus during conscious recollection in schizophrenia. Nat. Neurosci. 1, 318–322.

Inada, K., Ishigooka, J., Anzai, T., Suzuki, E., Miyaoka, H., Saji, M., 2003. Antisense hippocampal knockdown of NMDA-NR1 by HVJ-liposome vector induces deficit of prepulse inhibition but not of spatial memory. Neurosci. Res. 45, 473–481.

Iwakuma, M., Anzai, T., Kobayashi, S., Ogata, M., Kaneda, Y., Ohno, K., Saji, M., 2003. Antisense in vivo knockdown of synaptotagmin I and synapsin I by HVJ-liposome mediated gene transfer modulates ischemic injury of hippocampus in opposing ways. Neurosci. Res. 45, 285–296.

Javitt, D.C., Zukin, S.R., 1991. Recent advances in the phencyclidine model of Schizophrenia. Am. J. Psychiatry 148, 1301–1308.

Kaneda, Y., 1999. Development of a novel fusogenic viral liposome system (HVJ-liposomes) and its applications to the treament of acquired diseases. Mol. Memb. Biol. 16, 119–122.

Keller, A., 2002. Use-dependent inhibition of dendritic spines. Trends Neurosci. 25, 541–544.

Kobayashi, S., Ohno, K., Iwakuma, M., Kaneda, Y., Saji, M., 2002. Synaptotagmin I hypothalamic knockdown prevents amygdaloid seizure-induced damage of hippocampal neurons but not of entorhinal neurons. Neurosci. Res. 44, 455–465.

Lendvai, B., Stern, E.A., Chen, B., Svoboda, K., 2000. Experience-dependent plasticity of dendritic spines in the developing rat barrel cortex in vivo. Nature 404, 876–881.

Malhotra, A.K., Pinals, D.A., Adler, C.M., Elman, I., Clifton, A., Pickar, D., Breier, A., 1997. Ketamine-induced exacerbation of psychotic symptoms and cognitive impairment in neuoleptic-free schizophrenics. Neuropsychopharmacology 17, 141–150.

Marrs, G.S., Steven, H.G., Dailey, M.E., 2001. Rapid formation and remodeling of postsynaptic dendrites in developing dendrites. Nat. Neurosci. 4, 1006–1013.

Morris, R.G., Garrud, P., Rawlins, J.N.P., O'Keef, J., 1982. Place navigation impaired in rats with hippocampal lesions. Nature 297, 681–683.

Okabe, S., Miwa, A., Okado, H., 2001. Spine formation and correlated assembly of presynaptic and postsynaptic molecules. J. Neurosci. 21, 6105–6114.

Saeki, Y., Matsumoto, N., Nakano, Y., Mori, M., Awai, K., Kaneda, Y., 1997. Development and characterization of cationic liposomes conjugated with HVJ (Sendai virus): reciprocal effect of cationic lipid for in vitro and in vivo gene transfer. Hum. Gene Ther. 8, 2133–2144.

Shim, K.S., Lubec, G., 2002. Drebrin, a dendritic spine protein, is manifold decreased in brains of patients with Alzheimer's disease and Down syndrome. Neurosci. Lett. 324, 209–212.

Shirao, T., Obata, K., 1986. Immunochemical homology of 3 developmentally regulated brain proteins and their developmental change in neuronal distribution. Brain Res. 394, 233–244.

Shirao, T., Inoue, H.K., Kano, Y., Obata, K., 1987. Localization of a developmentally regulated neuron-specific protein S54 in dendrites as revealed by immunoelectron microscopy. Brain Res. 413, 374–378.

Shirao, T., Hayashi, K., Ishikawa, R., Isa, K., Asada, H., Ikeda, K., Uyemura, K., 1994. Formation of thick curving bundles of actin by drebrin A expressed in fibroblasts. Exp. Cell Res. 215, 145–153.

Shirao, T., 1995. The roles of microfilament-associated proteins, drebrins, in brain morphogenesis: a review. J. Biochem. (Tokyo) 117, 231–236.

Shirao, T., Sekino, Y., 2001. Clustering and anchoring mechanisms of molecular constituents of postsynaptic scaffolds in dendritic spines. Neurosci. Res. 40, 1–7.

Takahashi, H., Sekino, Y., Tanaka, S., Mizui, T., Kishi, S., Shirao, T., 2003. Drebrin-dependent actin clustering in dendritic filopodia governs synaptic targeting of postsynaptic density-95 and dendritic spine morphogenesis. J. Neurosci. 23, 6586–6595.

Tanaka S., Sekino Y., Shirao, T., 2001. Change of dendritic spine length induced by drebrin A knockdown using antisense oligonucleotides in vitro. Soc. Neurosci. Abstr. 29.

Wiser, A.K., Andreasen, N.C., O'Learly, D.S., Watkins, G.L., Boles Ponto, L.L., Hichwa, R.D., 1998. Dysfunctional cortico-cerebellur circuits cause 'cognitive dysmetria' in schizophrenia. Neuroreport 9, 1895–1899.

Yamada, K., Moriguchi, A., Morishita, R., Aoki, M., Mikami, H., Oshima, T., Ninomiya, M., Kaneda, Y., Higaki, J., Ogihara, T., 1996. Efficient oligonucleotide delivery using the HVJ-liposome method in the central nervous system. Am. J. Physiol. 271, R1212–R1220.

Zapata, A., Capdevilla, J.L., Tarrason, G., Martinez, J.M., Piulats, J., Trulla, R., 1997. Effects of NMDA-R1 antisense oligonucleotides administration: behavioral and radioligand binding studies. Brain Res. 745, 114–120.

Current Biology, Vol. 14, 650–658, April 20, 2004, ©2004 Elsevier Ltd. All rights reserved. DOI 10.1016/j.cub.2004.03.063

Drebrin Is a Novel Connexin-43 Binding Partner that Links Gap Junctions to the Submembrane Cytoskeleton

Eugenia Butkevich,[1,2] Swen Hülsmann,[1,2] Dirk Wenzel,[3] Tomoaki Shirao,[4] Rainer Duden,[5,*] and Irina Majoul[3,5,*]
[1]Department of Neurophysiology
University of Göttingen
Germany
[2]Research Centre Molecular Physiology of the Brain
Göttingen
Germany
[3]Department of Neurobiology
Max-Planck-Institute for Biophysical Chemistry
Göttingen
Germany
[4]Department of Neurobiology and Behavior
Gunma University Graduate School of Medicine
Maebashi
Japan
[5]Cambridge Institute for Medical Research
University of Cambridge
Cambridge
United Kingdom

Summary

Background: Connexins form gap junctions that mediate the transfer of ions, metabolites, and second messengers between contacting cells. Many aspects of connexin function, for example cellular transport, plaque assembly and stability, and channel conductivity, are finely tuned and likely involve proteins that bind to connexins' cytoplasmic domains. However, little is known about such regulatory proteins. To identify novel proteins that interact with the COOH-terminal domain of Connexin-43 (Cx43), the most widely expressed connexin family member, we applied a proteomics approach to screen fractions of mouse tissue homogenates for binding partners.

Results: Drebrin was recovered as a binding partner of the Cx43 COOH-terminal domain from mouse brain homogenate. Drebrin had previously been described as an actin binding protein that diminishes in brains during Alzheimer's disease. The novel Drebrin-Cx43 interaction identified by proteomics was confirmed by colocalization of endogenous proteins in astrocytes and Vero cells, coimmunoprecipitation, electron microscopy, electrophysiology, coexpression of both proteins with fluorescent tags, and live-cell FRET analysis. Depletion of Drebrin in cells with siRNA results in impaired cell-cell coupling, internalization of gap junctions, and targeting of Cx43 to a degradative pathway.

Conclusions: We conclude that Drebrin is required for maintaining Cx43-containing gap junctions in their functional state at the plasma membrane. It is thus possible that Drebrin may interact with gap junctions in zones of cell-cell contacts in a regulated fashion in response to extracellular signals. The rearrangement or disruption of interactions between connexins and the Drebrin-containing submembrane cytoskeleton directs connexins to degradative cellular pathways.

*Correspondence: im266@cam.ac.uk (I.M.), rd217@cam.ac.uk (R.D.)

Introduction

Gap junctions are transmembrane channels between contacting cells and mediate intercellular communication and signaling by permitting the passage of ions, metabolites, and second messengers [1–3]. Connexins organize themselves into hexameric assemblies, named hemi-channels or connexons, that contain six subunits. After transport to the plasma membrane, connexons can align between neighboring cells head-to-head to form the functional and regulated gap junction channels. More than 20 connexin isoforms encoded by different genes have been described in the human genome [4], allowing the synthesis of a large number of channels with different functional properties. All connexins comprise four transmembrane helices, two extracellular loops rigidly held together by disulfide linkages, and three variable cytoplasmic domains: amino terminus, cytoplasmic loop, and carboxy terminus [1]. The importance of gap junctions for multicellular organisms is highlighted by a wide array of different human diseases and mouse phenotypes that arise from defects in these genes. In mice null mutations in Cx43, the main connexin of gap junctions in heart and many other tissues, cause death shortly after birth. The hearts of such mice beat, but a malformation of their heart is fatal. In humans, the inherited defects in individual connexin isoforms are associated with demyelinating disorders of the peripheral nervous system, severe hearing impairment, eye lens cataracts, skin disorders, heart arrhythmias, and heart malformation [4]. Some of these diseases have a significant impact on the human population, with Cx26 mutations accounting for more than 50% of the cases of inherited asyndromic sensorineural deafness [4]. The intracellular transport of connexins, connexon assembly and channel formation, gap junction plaque assembly at the plasma membrane, and modulation of channel activities are most likely governed by interactions with regulatory and structural proteins that recognize specific sequence motifs in the cytoplasmic domains of connexins. However, only a few such connexin-interacting proteins have been described to date, and these include the tight junction protein ZO-1, tubulin, and the kinase c-Src [5–8].

In this study we screened for new interaction partners of Cx43, the most widely expressed member of the connexin family. We identified Drebrin as a novel interaction partner of the Cx43 COOH-terminal domain at the plasma membrane. Drebrin, previously described as an actin binding protein [9], was recovered from mouse brain homogenates. We confirmed the importance of Cx43/Drebrin interaction in living cells and analyzed the effects of RNAi depletion of Drebrin on gap junction

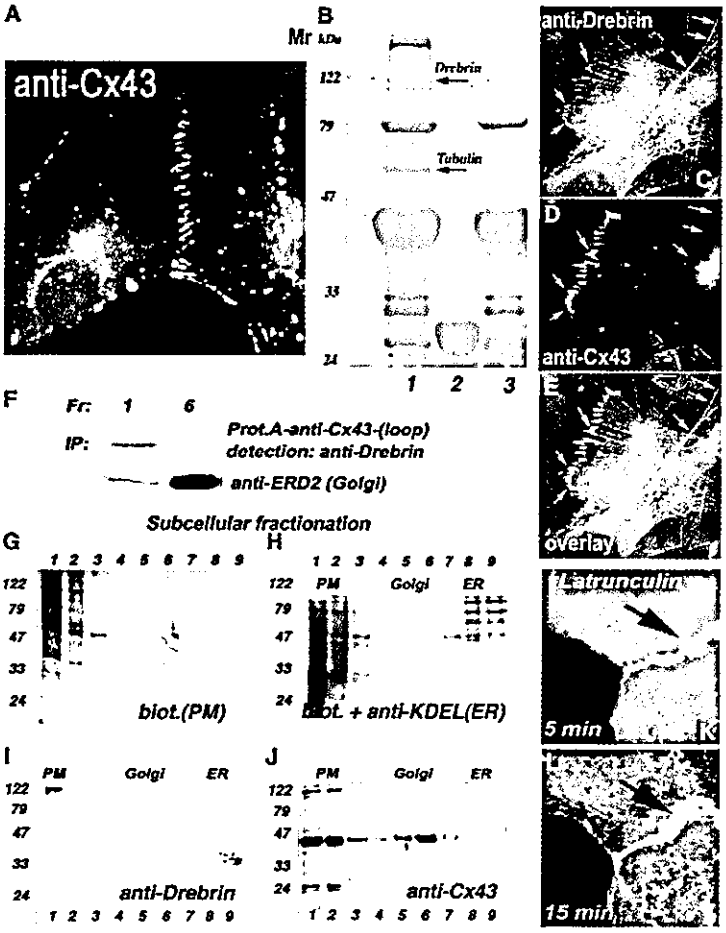

Figure 1. Drebrin Interacts with Connexin-43 In Vitro and Colocalizes with Connexin-43 at the Plasma Membrane by Immunofluorescence

(A) Distribution of endogenous connexin-43 in astrocytes.

(B) SDS-PAGE and Coomassie staining of proteins obtained in a pull-down assay with a GST-fusion protein encompassing the Cx43-COOH-terminal domain (residues 234–382) with a membrane fraction of mouse brain homogenate. Arrows indicate the positions of Drebrin and tubulin. Both proteins were identified by MALDI-Q-TOF in the pull-down fraction.

(C–E) Plasma membrane colocalization of endogenous Drebrin E and Cx43 in astrocytes as detected with anti-Cx43 and anti-Drebrin M2F6 antibodies, respectively. In the noncontacting regions of the plasma membrane, Drebrin E does not colocalize with Cx43.

(F–J) Subcellular fractionation of Vero cells and characterization of the separated fractions. (F) anti-Cx43 antibodies (raised against the first extracellular loop) immobilized on protein A Sepharose can coimmunoprecipitate Drebrin from the plasma membrane fraction (1). Anti-ERD2 antibodies (used as a control of the Golgi fractions) show the relative distribution of transmembrane Golgi protein in fractions 1 and 6. (G) Fractions containing biotinylated proteins, corresponding to the plasma membrane (PM), were detected with streptavidin-peroxidase. (H) A blot probed with streptavidin-peroxidase (fractions 1–3) was again exposed to anti-KDEL antibodies to reveal the ER (fractions 8 and 9). (I) Drebrin was detected in the pellet of the plasma membrane fraction. (J) Cx43 was present in both plasma membrane and the Golgi fractions.

(K and L) Time-dependent accumulation of Drebrin under the plasma membrane of Vero cells transfected with CFP-Drebrin and Cx43-YFP upon Latrunculin B treatment.

stability and permeability. Our data indicate that Drebrin is required to maintain functional Cx43-containing gap junctions at the cell surface.

Results and Discussion

Pull-Down Assays with the Cx43 COOH-Terminal Domain Recover Drebrin from Brain Homogenate

In search of new interaction partners of Cx43, we used a proteomics approach to screen subcellular fractions from different mouse tissues (brain, kidney, lung, heart, and liver) for proteins that may interact with a GST-fusion protein encompassing the Cx43 COOH-terminal domain (residues 234–382), which is normally exposed to the cytosol. Pull-down assays with this Cx43-COOH terminal domain fusion protein recovered several bands that were resolved by SDS-PAGE and visualized with Coomassie Blue (Figure 1B). MALDI/Q-TOF (matrix-assisted laser desorption ionization/quadrupole time-of-flight) mass spectrometry analysis of tryptic peptides identified a number of these proteins. One of them, Drebrin E, was reproducibly recovered in pull-down assays from the brain membrane fraction via the Cx43-GST fusion protein (Figure 1B). Drebrin has been previously described as an actin binding protein [9] whose level is greatly decreased in brains of Alzheimer patients [10]. We obtained 22 peptides by Q-TOF sequence analysis with exact matches to the cDNA-derived protein sequence of Drebrin ($p < 0,05$) (see Table S1 in the Supplemental Data available with this article online).

Another band obtained in the pull-down assay was identified by MALDI Q-TOF analysis as β-tubulin (see arrow in Figure 1B; peptide data not shown), which has already been described as an interaction protein for Cx43 [7]. A further previously described Cx43 binding partner, the tight-junction protein ZO-1 [5, 6], was present in the starting plasma membrane fractions, as detected by immunoblots with a ZO-1 antibody. Nevertheless, ZO-1 was not recovered on the Cx43-GST fusion protein under our experimental conditions, which included the presence of 1% Triton and ATP in the binding reactions and wash buffer.

Next we analyzed the distribution of endogenous Drebrin E and Cx43 by immunofluorescence with the corresponding antibodies. In astrocytes (Figures 1C–1E) and Vero cells (Figures 3A and 3B), a clear colocalization of

both proteins underneath the plasma membrane in the region of cell-cell contacts was observed. On the other hand, inside the cell and in noncontacting regions of the plasma membrane, Drebrin E did not colocalize with Cx43 (Figures 1C–1E, 3A, and 3B).

Subcellular fractionation of Vero cells, performed as we described previously [11] and in the Supplemental Data available with this paper online, revealed that Cx43 was present in both the plasma membrane (PM) and Golgi fractions (Figure 1J), whereas Drebrin was detected only in the plasma membrane fraction (Figure 1I). Fractions containing Golgi membranes were detected by an enzyme assay for UDP-galactosyltransferase, and the plasma membrane fractions were recognized by streptavidin-peroxidase after cell-surface biotinylation of intact cells on ice (Figure 1G), as described by us previously [11]. Golgi fractions in the gradient were detected with antibodies against the transmembrane Golgi KDEL-receptor (ERD2). ER fractions were recognized by the maximal activity of Rotenone-insensitive cytochrome-C reductase [11] in gradient fractions and with antibodies directed against the KDEL-peptide sequence (which is characteristic for many ER resident lumenal proteins) in immunoblots (Figure 1H; fractions 8 and 9). Immunoprecipitations with anti-Cx43 antibodies (raised against the first external loop, residues 46–68) were performed from the fractions, and immunoblotting with anti-Drebrin antibodies allowed analysis of coprecipitating proteins. Drebrin was immunoprecipitated from the PM fraction but not from the Golgi fractions (Figure 1F). These results confirm that Drebrin is associated with Cx43 in the plasma membrane fraction.

To test whether the submembrane localization of Drebrin depends on the presence of polymerized actin, we treated Vero cells with the actin-depolymerizing drug Latrunculin B (100 nM). In Vero cells transfected with CFP-Drebrin and Cx43-YFP, Drebrin was still detected underneath the PM of contacting cells after Latrunculin B treatment and thus was not dispersed through the cytoplasm in the absence of actin filaments (Figures 1K and 1L).

Live-Cell Analyses Reveal Drebrin/Cx43 Interactions in Submembrane Regions of Cell-Cell Contacts

Live-cell imaging of COS cells expressing CFP-Drebrin and Cx43-YFP revealed that Drebrin strongly accumulates in contacting regions of the plasma membranes only when Cx43 is present there (Figure 2A–2C). To confirm the close molecular proximity of Drebrin and Cx43 in the regions of cell-cell contacts, we used live-cell fluorescence resonance energy transfer (FRET) and an acceptor bleach protocol that we had developed earlier [12, 13]. For these experiments, CFP-Drebrin and Cx43-YFP were coexpressed in Vero cells. In case of FRET proximity, the photoinactivation of the acceptor (Cx43-YFP) results in an increase of the fluorescence of the donor (CFP-Drebrin). First, donor and acceptor images were acquired as follows: donor before bleach (Dbb) and acceptor before bleach (Abb) (Figures 2D and 2E). Photoinactivation of the acceptor (Cx43-YFP) was performed with an external laser at λ_{ex} 530 nm, and images were acquired as follows: acceptor after bleach (Aab) and donor after bleach (Dab). In the regions of cell-cell contacts containing CFP-Drebrin and Cx43-YFP, a clear FRET signal was revealed by an increase in the donor fluorescence (CFP-Drebrin) after the acceptor (Cx43-YFP) was photoinactivated (Figures 2F and 2G).

For a more precise characterization of the CFP-Drebrin/Cx43-YFP interaction underneath the plasma membrane, we analyzed the comparative degree of the donor dequenching along the interface of contacting cells upon direct photoinactivation of the acceptor (Cx43-YFP) by using image data processing with the MetaMorph 6.0 program (Figure 2H). The comparison of two graphs derived from the same cellular region obtained before (Dbb) and after (Dab) acceptor inactivation revealed a 15%–25% increase in the donor fluorescence (small arrows in zones of cell-cell contacts in Figure 2H). As a negative control, the unchanged background region of the same cell is depicted before and after the acceptor bleach (big arrows in Dbb and Dab, Figure 2H). The degree of acceptor photoinactivation in each pixel along the linescan is shown in Figure 2H (Abb, Aab). 3D reconstruction of the profile scan revealed the distribution of FRET between CFP-Drebrin and Cx43-YFP underneath the plasma membrane (Figure 2I).

We further confirmed FRET proximity between CFP-Drebrin and Cx43-YFP by using a Zeiss LSM 510 META microscope setup. CFP-Drebrin and Cx43-YFP interactions were analyzed in living cells during the time-dependent photoinactivation of the acceptor in the region of cell-cell contacts where both donor and acceptor were present (Figure 2J). The time-dependent increase in the donor fluorescence (CFP-Drebrin) was inversely proportional to the degree of acceptor (Cx43-YFP) inactivation (Figure 2K). All images are representative of at least three independent sets of experiments and confirm that the interaction between Drebrin E and Cx43 occurs in the region of cell-cell contact in a living cell.

Disruption of Drebrin/Cx43 Interactions by Drebrin RNAi Directs Cx43 for Degradation

To better understand the functional importance of the Drebrin/Cx43 interaction in a live cell, we decreased the level of Drebrin in Vero cells by using transfection with siRNA duplex oligos directed against Drebrin (see Experimental Procedures and [14]). In control cells, Drebrin E and Cx43 were colocalized in the regions of cell-cell contact by immunofluorescence (Figures 3A and 3B). Forty-eight hours after oligofectamine transfection with the siRNA oligos against Drebrin, we observed a significant decrease in both the immunoblot (Figure 3M) and immunofluorescence signals with anti-Drebrin antibodies (compare Figures 3A and 3D). Drebrin siRNA-silenced cells showed a strong decrease of the staining for Cx43 (Figure 3E). In control Vero cells transfected with Cx43-GFP, immunoelectron microscopy with antibodies against Drebrin or Cx43 revealed that both proteins are present in plasma membrane regions containing gap junctions (Figure 3C). We observed that transfection with Drebrin siRNA induced the scattering of Cx43-GFP through the cytoplasm (Figure 3G). Immunoelectron microscopy analysis of Vero cells transfected with Drebrin

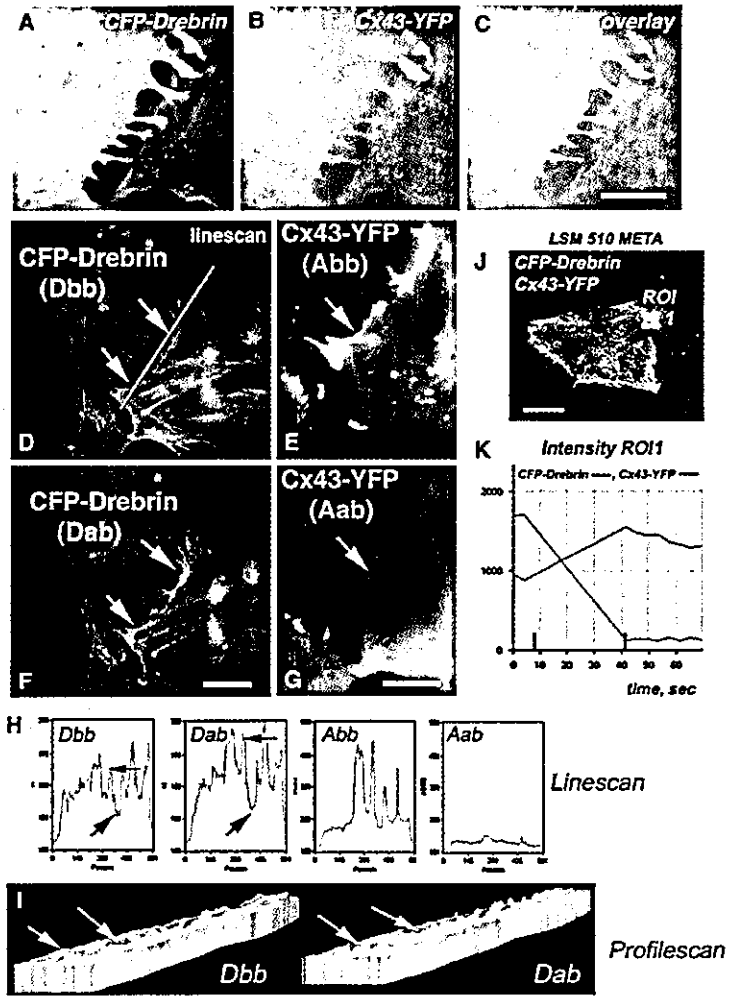

Figure 2. CFP-Drebrin and Cx43-YFP Colocalize in Living Cells and Show a FRET Interaction

(A–C) COS cells transfected with CFP-Drebrin and Cx43-YFP reveal strong colocalization of both proteins in the regions of cell-cell contacts. Note that CFP-Drebrin also accumulates in regions of cell-cell contact where Cx43-YFP is present.

(D–K) FRET analyses of live Vero cells expressing CFP-Drebrin/Cx43-YFP. (D and E) Donor (Dbb) and acceptor (Abb) images before acceptor inactivation. (F and G) Donor (Dab) and acceptor (Aab) images after acceptor photoinactivation done with an external laser at λ_{ex} 530 nm. (H) corresponding linescans (Dbb, Dab, Abb, Aab) along the cell-cell interface; small arrows indicate an increase in donor fluorescence, and big arrows show the unchanged background. (I) 3D reconstruction of a profile scan shows the distribution of FRET between CFP-Drebrin and Cx43-YFP under the plasma membrane (compare Dab to Dbb). (J and K): FRET between CFP-Drebrin and Cx43-YFP detected with the LSM 510 META microscope setup. The diagram shows that the time-dependent increase in donor fluorescence (CFP-Drebrin, green) is inversely proportional to the degree of acceptor (Cx43-YFP, red) inactivation (K).

siRNA revealed the presence of Cx43 in multivesicular intracellular membrane structures inside the cell (Figure 3F), most likely indicating that this connexon material had undergone internalization and was subject to degradation. This contrasts with a prominent cell-cell contact pattern observed in control cells (Figure 3C). Microinjection of calcein into Vero cells transfected with Drebrin siRNA resulted in a decreased ability to transfer dye to the neighboring cells as compared to the control cells (Figure 3K and 3L).

The results show that in Drebrin siRNA transfected cells the connexons are not able to maintain functional gap junctions, resulting in a decreased transfer of calcein to the surrounding cells. The decrease in the endogenous Drebrin level in siRNA-transfected Vero cells also resulted in a dramatic decrease of the endogenous Cx43 level compared to that of the control cells (Figure 3M); this decrease correlates well with the disappearance of Cx43 from the submembrane zones of cell-cell contacts. Furthermore, in actin-GFP-expressing cells we observed extensive ruffling of the plasma membrane after transfection with Drebrin siRNA that was not observed in control cells (Figures 3I and 3J).

Functional Stabilization of Gap Junctions in Astrocytes on the Plasma Membrane by Drebrin May Favor Increased Cell-Cell Coupling and Dye Transfer

We examined the cell-cell coupling in astrocytes and Vero cells by using electrophysiology and dye transfer. Compared to Vero cells (Figure 4B), astrocytes showed strong cell coupling (Figure 4A). We compared the localization of endogenous Cx43 and Drebrin in both cell types by immunofloresence with anti-Cx43 and anti-Drebrin antibodies. Astrocytes showed strong staining of the plasma membrane for Cx43 (Figure 4C, see also Figures 1C and 1D). In Vero cells endogenous Cx43 showed weaker staining of the plasma membrane and pronounced labeling of the Golgi region (Figure 4D). Plasma membrane localization of Cx43 in astrocytes (Figure 4C) correlates with stronger electrical coupling (Figure 4A) compared to that in Vero cells (Figure 4B). Cx43-GFP transfected into Vero cells localizes to the cell-cell interfaces (Figure 4B, upper right panel) and favors increased cell-cell coupling (data not shown). Cotransfection of Vero cells with Cx43-GFP and siRNA against Drebrin prevented the appearance of Cx43-GFP

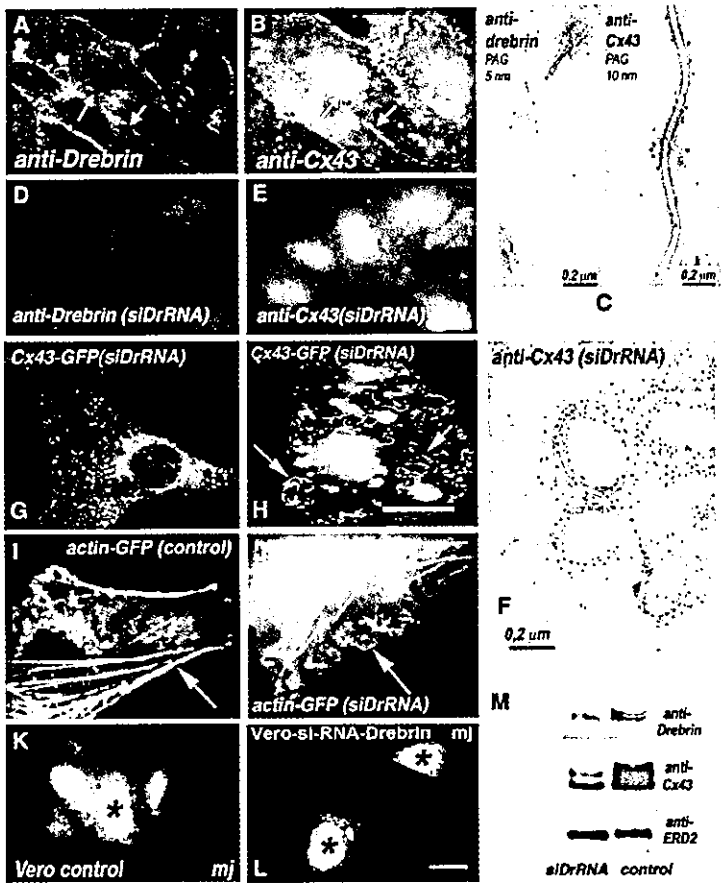

Figure 3. Cx43 in Cells Treated with Drebrin siRNA

(A and B) Distribution of endogenous Drebrin and Cx43 in Vero cells as revealed by immunofluorescence with anti-Drebrin and anti-Cx43 antibodies. Both proteins colocalize under the plasma membrane but do not colocalize in the Golgi region (see the arrows).

(C) The distribution of CFP-Drebrin and Cx43-YFP in Vero cells as detected by immunoelectron microscopy. Note that in Vero cells (which do not have tight junctions, desmosomes, or adherens junctions) Drebrin is present in regions of cell-cell contact with a gap junction appearance.

(D and E) Localization of Drebrin and Cx43 detected 48 hr after transfection of Vero cells with siRNA against Drebrin; the same antibodies as in (A) and (B) were used for detection. Note that the decrease in the level of Drebrin correlates with the decrease of Cx43 immunoreactivity and disappearance of Cx43 from the submembrane zones of cell-cell contacts.

(F) Formation of Cx43-GFP-containing multimembrane clusters in Vero cells cotransfected with siRNA against Drebrin (16 hr) was detected by immunoelectron microscopy with anti-GFP antibody.

(G) Scattering of Cx43-GFP through the cytoplasm in Vero cells transfected first with siRNA against Drebrin (24 hr) and then by Cx43-GFP transfection (10 hr).

(H) Vero cells cotransfected with siRNA against Drebrin and Cx43-GFP (10 hr).

(I and J) Vero cells transfected with GFP-Actin (I) or cotransfected with siRNA directed against Drebrin and GFP-Actin (J). The absence of Drebrin also induces ruffling of the plasma membrane (shown at 10 hr after transfection).

(K and L) Calcein transfer between control (K) and siRNA-Drebrin-transfected (l) cells 20 min after microinjection.

(M) Immunoblot analysis of Vero cells transfected with siRNA against Drebrin. Note that the decrease in Drebrin level results in a dramatic reduction of the level of Cx43 compared to that in control cells. Anti-ERD2 antibodies were used as a loading control.

in regions of cell-cell interfaces. Instead, Cx43-GFP staining was detected throughout the cytoplasm in small punctate structures and in a perinuclear region (Figure 4B, lower right panel).

We used double whole-cell voltage clamp recordings of a pair of primary cultured mouse astrocytes to analyze the state of cell-cell contact permeability (Figure 4E). One cell of the pair was exposed to voltage pulses of 200 ms with a holding potential at −70 mV in 10 mV increments (cell 1), whereas the adjacent cell was kept at −70 mV (cell 2). Current responses from both cells, i.e., the stimulated cell (I_1) and the neighboring cell coupled through the gap junctions (I_2) to the first cell, were recorded.

Comparison of the currents that pass through the gap junctions (I_2) of control cells, of cells cotransfected with Drebrin siRNA and a plasmid encoding the transmembrane Golgi protein p23-CFP, or of control cells transfected with just the p23-CFP plasmid revealed a strong decrease in cell-cell permeability in Drebrin siRNA-transfected astrocytes (Figure 4E). The fact that this effect was reproducible indicates that siRNA-mediated depletion of Drebrin strongly decreases cell-cell permeability, an observation that was confimed by stastistical evaluation (n = 6 for control cells and n = 5 for cells transfected with Drebrin siRNA) (Figure 4E, right panel). After siRNA-mediated depletion of Drebrin, calcein transfer between astrocytes (Figures 4G and 4H) was also strongly decreased from that in control astrocytes (Figure 4F), although the overall level of dye transfer even in Drebrin-depleted astrocytes still remained higher than in Vero control cells (data not shown).

Cx43 is a protein that is known to be phosphorylated on both serine and tyrosine residues, which changes its mobility upon SDS-PAGE [15, 16, 17]. Normally, in immunoblots of cultured mouse astrocytes, the anti-Cx43 antibodies show predominantly the upper, phosphorylated bands of Cx43 (Figure 4C, lower panel), and in Vero cells they show predominantly the lower, nonphosphorylated band (Figure 4D, lower panel). After partial depletion of Drebrin in cultured astrocytes by Drebrin siRNA, we detected fewer of the phosphorylated upper bands of Cx43 with anti-Cx43 antibodies (Figure 4C, lower panel). The functional consequences of Cx43 phosphorylation have been widely debated [15, 16].

Recently, Faucheux and coworkers, using inhibitors

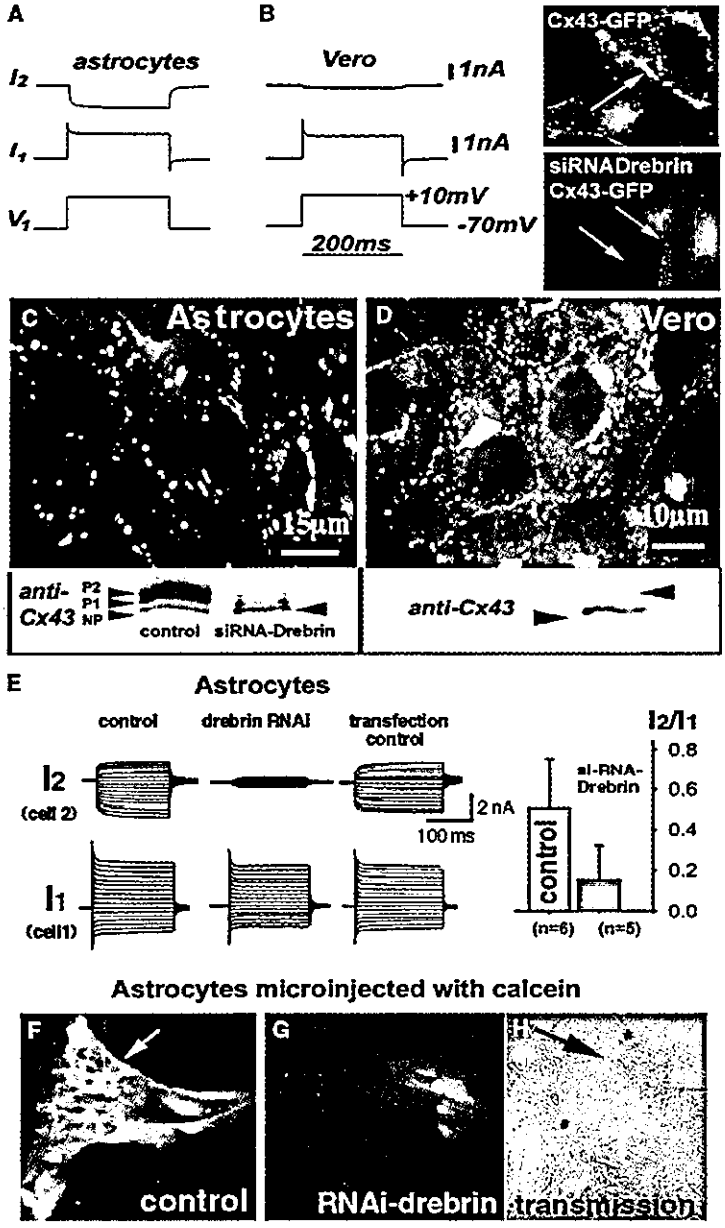

Figure 4. Drebrin Depletion by siRNA in Astrocytes Results in Reduced Electrical Coupling and Reduced Dye Transfer and Correlates with Loss of Cx43 Phosphorylated Bands

(A and B) A voltage step from −160 to +10 mV was applied to cell 1 while its contacting cell, cell 2, was kept at −70 mV. Current responses from stimulated cell 1 (I1) and from the neighboring cell 2 (I2) were recorded. Note that current response in astrocytes is always stronger than in Vero cells. Right: Vero cells transfected with Cx43-GFP and Cx43-GFP/siRNA Drebrin. Note that depletion of Drebrin facilitates the removal of connexins from the plasma membrane ([B], right panel) and thus decreases cell-cell coupling.

(C and D) Astrocytes and Vero cells reveal different cellular distribution of endogenous Cx43. Strong staining of the plasma membrane can be seen in astrocytes, whereas in Vero cells endogenous Cx43 showed only a punctate staining of the plasma membrane and a distinct labeling of Golgi membranes. Immunoblot with anti-Cx43 antibodies shows predominantly the phosphorylated upper bands of Cx43 in astrocytes and predominantly nonphosphorylated lower bands in Vero cells. After partial depletion of Drebrin in cultured astrocytes with siRNA, fewer upper phosphorylated bands of P1 and P2 of Cx43 can be detected.

(E) Double whole-cell voltage clamp recordings of a pair of primary-culture mouse astrocytes. Currents from the stimulated cell (I1) and currents that pass through the gap junctions (I2) were recorded from control cells, cells cotransfected with siRNA against Drebrin plus a control plasmid encoding the transmembrane Golgi protein p23-CFP, or cells transfected with the p23-CFP plasmid alone [11]. One cell of the pair was exposed to voltage pulses of 200 ms with a holding potential of −70 mV in 10 mV increments (cell 1), and the adjacent cell was kept at −70 mV (cell 2). Cells transfected with siRNA against Drebrin were recognized by the p23-CFP signal and by Cy-3 label of the oligos. Three representative cells are shown together with a statistical evaluation (n = 5 for control cells and n = 6 for cells transfected with Drebrin siRNA). Control astrocytes: I2/I1 = 0.517 ± 0.27 (n = 6); RNAi Drebrin: I2/I1 = 0.14 ± 0.03 (n = 5), p = 0.004.

(F) Astrocytes microinjected with calcein display the transfer of dye to the adjacent cells within seconds via the functional gap junctions.

(G and H) There is a strong decrease in calcein transfer observed in astrocytes transfected with Drebrin siRNA (G), although contacting cells are clearly visible in the transmission light image.

of cAMP protein kinase (PKA) and protein kinase C (GF109203X), showed a correlation between disappearance of Cx43 phosphorylated bands and a strong decrease in gap-junctional permeability [17]. Similarly, we saw a reduction of the P2 and P1 bands of Cx43 in astrocytes after siRNA-mediated Drebrin depletion (Figure 4C, lower panel). Therefore, it is tempting to speculate that Drebrin in astrocytes (most likely in complex with other submembrane proteins) may favor the functional stabilization of Cx43 at the plasma membrane. A reduction in the cellular level of Drebrin will destabilize Cx43 and may (directly or indirectly) influence other connexins that are expressed in astrocytes. Depletion of Drebrin facilitates the removal of connexins from the plasma membrane (as we observed for Cx43-GFP after siRNA-mediated Drebrin depletion in Vero cells; Figure 4B, right panel) and thus decreases cell-cell coupling.

Drebrin May Serve as a Linker between Cx43 and the Submembrane Cytoskeleton

In this paper we have demonstrated that Drebrin, which we found by a proteomics screen in a brain homogenate

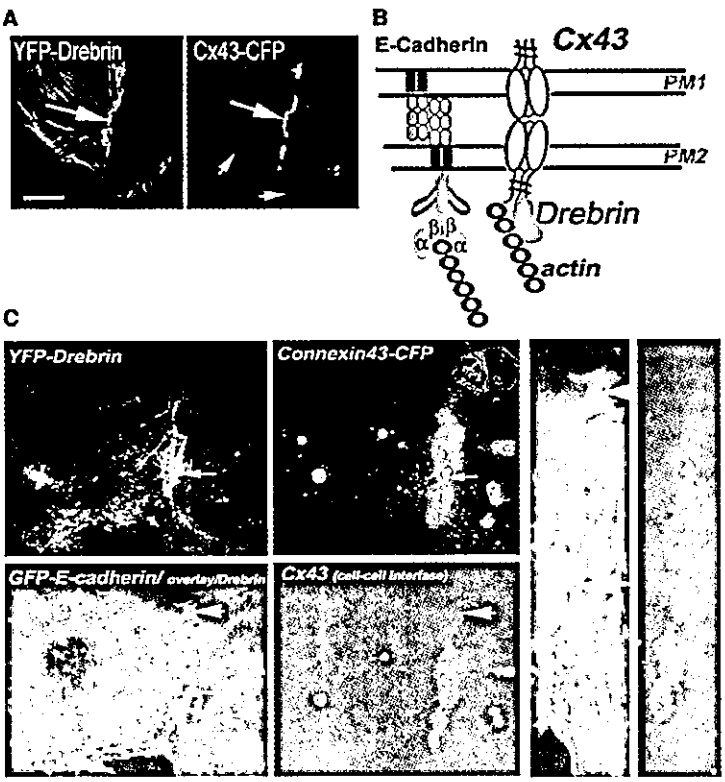

Figure 5. Intracellular Function of the Drebrin/Cx43 Interaction

(A) In Vero cells cotransfected with CFP-Drebrin and Cx43-YFP, both proteins are colocalized under the plasma membrane in the region of cell-cell contacts (big arrows) but not underneath the noncontacting plasma membrane regions (small arrows).

(B) Model introducing a comparison between the E-Cadherin/β-catenin/α-catenin/actin system and the novel Cx43/Drebrin/actin interactions discussed here.

(C) Plasma membrane interface of two cells cotransfected with Cx43-CFP, GFP E-cadherin, and CFP-Drebrin. Cx43-CFP is located mainly in the middle of the cell-cell interface, whereas GFP-E-cadherin is present mainly at the distal parts of the cell-cell interface. Drebrin is preferentially localized in the region labeled by Cx43-CFP and less in the distal parts labeled by GFP-E-cadherin.

fraction, not only colocalizes with Cx43 underneath the plasma membrane but also interacts with the C-terminal domain of Cx43 in a living cell, as analyzed by FRET (Figure 2). Drebrin and Cx43 cotransfected into Vero cells with fluorescent tags (CFP and YFP, respectively) were both present in zones of cell-cell contact (Figures 2A–2C and 5A). Initially, Drebrin had been described as an actin binding protein [18]. Additionally, a scaffolding role of Drebrin in the submembrane cytoskeleton of dendritic spines has been documented [19, 20]. Precedents for the regulation and stabilization of cell-cell contacts via crucial interactions with cytoplasmic proteins, (e.g., cell-cell adhesion mediated by E-cadherin) are well described [21]. In light of this, we consider it likely that Drebrin functions as a linker between gap junctions and the actin/submembrane cytoskeleton. We hypothesize that there is an analogy between the E-cadherin/β-catenin/α-catenin/actin system [21, 22] and the Cx43/Drebrin/actin system (as depicted in Figure 5B). Cx43 as well as E-cadherin may be utilized not only for cell–cell contacts but also to convey extracellular signals to their intracellular effectors by using Drebrin for the modification of the submembrane cytoskeleton in response to extracellular stimuli. This function may be fulfilled by Cx43 hemichannels that exist in the noncontacting membranes. As a first step to address this, we compared the intracellular distribution of E-cadherin, Cx43, and Drebrin. We cotransfected Vero cells with GFP-E-cadherin, Cx43-CFP, and YFP-Drebrin and linearly separated the fluorescent signals. The distribution of GFP-E-cadherin and Cx43-YFP in transfected Vero cells revealed that the initial interface between two cells was defined by E-cadherin pointed cell-cell contacts, whereas Cx43 was not present at the initial points of cell-cell contact (data not shown here). After a stable cell-cell contact interface was established by E-cadherin, Cx43-CFP started to accumulate in the middle region of this cell-cell interface (Figure 5C). Finally, in established cell-cell contacts Drebrin colocalizes more with Cx43 than with E-cadherin, suggesting that the Cx43/Drebrin complex may laterally displace E-cadherin together with cadherin-interacting proteins to the distal parts of this cell-cell interface. One of the previously described interacting partners of Cx43 underneath the plasma membrane is ZO-1 [5, 6]. ZO-1 has also been reported to bind cadherin molecules that appear to regulate the translocation of ZO-1 to the cell surface through interaction with catenins [23, 24]. In cases where Cx43 and E-cadherin are segregated during the formation of cell-cell contact interfaces, the relative strength of these interactions will determine the cellular distribution of ZO-1.

Intriguingly, Drebrin levels have been shown decrease during Alzheimer's disease (AD) [10, 25]. Thus, our single-cell experiments with siRNA-mediated depletion of Drebrin may somehow mimic the decreased level of Drebrin in AD, causing increased degradation of Cx43 and consequently impairing cell-cell coupling. Interestingly, Cx43 immunoreactivity was elevated at sites of amyloid plaques of Alzheimer's patients [26]. Our data allow us to speculate that the increased Cx43 expression in AD may represent an attempt of tissues to main-

tain homeostasis by aberrant induction of Cx43 expression in the pathological microenvironment of amyloid plaques. A similar mechanism of induction has been recently described for β-catenin, whose level is boosted by the loss of the noncanonical Wnt pathway [27].

In this study, we provide evidence for Drebrin as a novel and important interacting partner of Cx43 at the plasma membrane and show that it stabilizes Cx43-containing gap junctions in their functional state. Once gap junction plaques were formed, CFP-Drebrin still colocalized with Cx43-YFP in Vero cells even after Latrunculin B treatment, suggesting that the presence of actin filaments is not crucial for the Drebrin/Cx43 interaction. Interestingly, in mature hippocampal neurons the PSD-95 clusters containing Drebrin are also insensitive to Latrunculin A, suggesting that PSD-95 distribution is independent of the actin cytoskeleton [31]. In contrast, in developing neurons the synaptic clustering is still sensitive to Latrunculin A [20].

Depletion of Drebrin causes Cx43 to be targeted to a degradative pathway. Potentially, the cytoplasmic C-terminal domain of Cx43 is a highly regulated region that contains multiple motifs for protein-protein interactions. Interaction partners will likely include different kinases and molecules that recognize the Cx43 COOH terminus in its phosphorylated state, molecules containing PDZ, SH2, and SH3 domains, and components of the cellular ubiquitination machinery. In a very simple model, during gap junction formation Drebrin may bind to the C-terminal domain of Cx43 and thus sterically prevent interactions with other modifying molecules. Alternatively, Drebrin may stabilize Cx43 in its functional state as part of a larger submembrane cytoskeleton complex.

Experimental Procedures

GST-COOH-Terminus-Cx43 Construct; GFP Constructs

To create the GST-COOH-Cx43 (amino acids 234–382) construct, the relevant part of rat Cx43 [28] amplified by PCR. The sequences of the primers were as follows: forward primer, 5′-CTAGGGATC CAAGGGCGTTAAGGATCGCGTGAAG-3′; and reverse primer, 5′-CTA GGCGGCCGCTTAAATCTCCAGGTCATCAGG-3′. The PCR product was restricted with Bam HI and Not I and ligated into the Bam HI/Not I sites of pGEX-4T-3 (Pharmacia). A cDNA encoding human Drebrin E (accession number D17530; [29]) was used for generation of the CFP-Drebrin construct. Cloning of PCR fragments was used for generation of the YFP-, CFP- and GFP-tagged versions of full-length rat Cx43 used in this study. All constructs were verified by DNA sequencing.

Expression and Purification of GST-COOH-Cx43 Protein; GST Pull-Down Assay

GST-COOH-Cx43 protein was expressed in *E. coli* XL1 blue cells at 24°C in the presence of 100 μM IPTG and purified on Glutathione Sepharose 4B beads.

A fresh mouse brain was homogenized with 2 ml of internal medium containing "Complete" protease inhibitor (Roche). The homogenate was centrifuged 45 min at 100,000 g_{av} at 4°C. The supernatant was used in experiments as the "cytosol fraction." The pellet was resuspended in 2 ml of the same buffer, containing Triton X-100 to 1%, and centrifuged as described. The supernatant was used in experiments as the "membrane fraction."

The brain fractions were precleared by incubation with 50 μg of GST for 2 hr at 4°C on a rotating platform. A 20% suspension of glutathione sepharose 4B beads (300 μl) was added after the first 1 hr of this incubation. The samples were centrifuged at 500 g for 3 min, and the supernatant was used. The precleared fractions were then incubated with 300 μl of Glutathione Sepharose 4B beads loaded with GST fusion protein for 1.5 hr at 4°C on a rotating platform. Beads were washed five times in internal medium, containing "Complete" protease inhibitors (Roche) and 1% Triton X-100. The samples were boiled for 2 min in 60 μl 2× SDS-PAGE sample buffer containing 0.1% β-mercaptoethanol. The liquid phases were collected, and proteins were separated on 12% SDS-PAGE gels.

siRNA

siRNA duplexes against human Drebrin E (also called Drebrin I) (5′-CCAGAAGGUGAUGUACGGCdTdT-3′ sense and 3′-dTdTGGUCU UCCACUACAUGCCG-5′antisense) "Option C," nonlabeled or labeled with Cy3 on the 5′ end of the sense strand, were produced by Dharmacon (http://www.Dharmacon.com/).

Cell Culture and Transfection

Vero (ATCC) as well primary cultures of astrocytes obtained from mice brain were used in experiments. Cells were maintained in Dulbecco's modified Eagles medium, supplemented with 10% fetal calf serum, penicillin/streptomycin (100 μg/ml), and L-glutamine (2 mM). Transfection of Vero cells was performed by electroporation [11]. Transiently transfected cells (6–16 hr) were used in experiments. Oligofectamine reagent (Invitrogen) was used for siRNA transfection according to the manufacturers' instructions. For cotransfection with siRNA and DNA, cells were electroporated as described earlier except that the buffer was prepared with deionized RNAase-free water. siRNA-transfection with Oligofectamine was followed 24 hr thereafter by transfection with Cx43-GFP or GFP-actin-encoding plasmids. Expression patterns were analyzed within 6–18 hr after transfection with plasmids.

Immunocytochemistry

To study the cellular distribution of endogenous Cx43 and Drebrin, we fixed Vero cells and astrocytes in 3% PFA in the presence of FCS, washed the cells, and then permeabilized them with 0.1% saponin/3% BSA in PBS. Commercial antibodies against Cx43 (Sigma C6219) and a monoclonal antibody M2F6 against Drebrin (Stressgen) were used in combination with Cy3- and Cy2-labeled secondary antibodies. Cells were mounted in Fluorosave (Calbiochem) and analyzed with a Zeiss Axiovert 100 microscope.

FRET Analyses

CFP-Drebrin (donor) and Cx43-YFP (acceptor) were coexpressed in Vero cells for 6–12 hr. FRET (acceptor bleach) was applied for analysis of donor-acceptor interactions as described previously [11, 12]. In brief, Dbb (donor before bleach) and Abb (acceptor before bleach) images were acquired with a Zeiss Axiovert 100 TV fluorescence microscope equipped with 100× 1.4 NA Plan Apochromate objective lens, a CCD camera (Kodak, Princeton Instruments), and CFP and YFP filter sets (Omega Optics and AF Analytic, Germany). An increase in donor fluorescence was monitored with an excitation filter set that consisted of the following: for excitation, BP 430/20; and for emission, BP 485/17. Images were analyzed with MetaMorph 6.0 (Universal Imaging Corporation, West Chester, PA). After acquisition of Dbb and Abb images, the acceptor was photoinactivated with a green laser λ_{ex} 530 nm built into the Zeiss Axiovert 100, and two other images, Dab (donor after bleach) and Aab (acceptor after bleach), were recorded.

Supplemental Data

Supplemental Data including additional Experimental Procedures (surface biotinylation and subcellular fractionation; immunoprecipitation; immunoelectron microscopy [30]) and a table (peptide summary report) are available with this article online at http://www.current-biology.com/cgi/content/full/14/8/650/DC1/.

Acknowledgments

We are grateful to K. Lilley (Cambridge Centre for Proteomics) for MALDI Q-TOF analysis used for protein identification. We thank H.-D. Söling for his support and helpful discussions, S. Elbashir and J. Harborth for assistance with the siRNA experiments, and K. Weber for helpful comments (all at the Max-Planck Institute for Biophysical

Chemistry, Göttingen, Germany). We thank G. Söhl, K.Willecke, and M. Falk for Cx43 plasmids, J. Nelson and R. Kemler for GFP-E-cadherin plasmids, S. Kuznetsov for the GFP-actin plasmid, comments, and support, and M. Dale (Cambridge, UK) for expert technical assistance. We also thank D. Goodenough for reading an early version of this manuscript and suggesting useful experiments and M.S. Robinson for critical reading of an advanced text version. This work was supported by the Wellcome Trust (Senior Fellowship to R.D.; grant number 047578), the Deutsche Forschungsgemeinschaft (DFG grant So 43/60-1), and a Sonderforschungsbereich 406 grant to S.H.

Received: December 8, 2003
Revised: February 26, 2004
Accepted: March 10, 2004
Published: April 20, 2004

References

1. Kumar, N.M., and Gilula, N.B. (1996). The gap junction communication channel. Cell *84*, 381–388.
2. Goldberg, G.S., Lampe, P.D., and Nicholson, B.J. (1999). Selective transfer of endogenous metabolites through gap junctions composed of different connexins. Nat. Cell Biol. *1*, 457–459.
3. Bukauskas, F.F., Jordan, K., Bukauskiene, A., Bennett, M.V., Lampe, P.D., Laird, D.W., and Verselis, V.K. (2000). Clustering of connexin 43-enhanced green fluorescent protein gap junction channels and functional coupling in living cells. Proc. Natl. Acad. Sci. USA *97*, 2556–2561.
4. Willecke, K., Eiberger, J., Degen, J., Eckardt, D., Romualdi, A., Guldenagel, M., Deutsch, U., and Sohl, G. (2002). Structural and functional diversity of connexin genes in the mouse and human genome. Biol. Chem. *383*, 725–737.
5. Toyofuku, T., Yabuki, M., Otsu, K., Kuzuya, T., Hori, M., and Tada, M. (1998). Direct association of the gap junction protein connexin-43 with ZO-1 in cardiac myocytes. J. Biol. Chem. *273*, 12725–12731.
6. Giepmans, B.N., and Moolenaar, W.H. (1998). The gap junction protein connexin-43 interacts with the second PDZ domain of the zona occludens-1 protein. Curr. Biol. *8*, 931–934.
7. Giepmans, B.N., Verlaan, I., Hengeveld, T., Janssen, H., Calafat, J., Falk, M.M., and Moolenaar, W.H. (2001). Gap junction protein connexin-43 interacts directly with microtubules. Curr. Biol. *11*, 1364–1368.
8. Giepmans, B.N., Hengeveld, T., Postma, F.R., and Moolenaar, W.H. (2001). Interaction of c-Src with gap junction protein connexin-43. Role in the regulation of cell-cell communication. J. Biol. Chem. *276*, 8544–8549.
9. Asada, H., Uyemura, K., and Shirao, T. (1994). Actin-binding protein, drebrin, accumulates in submembranous regions in parallel with neuronal differentiation. J. Neurosci. Res. *38*, 149–159.
10. Shim, K.S., and Lubec, G. (2002). Drebrin, a dendritic spine protein, is manifold decreased in brains of patients with Alzheimer's disease and Down syndrome. Neurosci. Lett. *324*, 209–212.
11. Majoul, I.V., Bastiaens, P.I., and Soling, H.D. (1996). Transport of an external Lys-Asp-Glu-Leu (KDEL) protein from the plasma membrane to the endoplasmic reticulum: studies with cholera toxin in Vero cells. J. Cell Biol. *133*, 777–789.
12. Majoul, I., Straub, M., Hell, S.W., Duden, R., and Soling, H.D. (2001). KDEL-cargo regulates interactions between proteins involved in COPI vesicle traffic: measurements in living cells using FRET. Dev. Cell *1*, 139–153.
13. Majoul, I., Straub, M., Duden, R., Hell, S.W., and Soling, H.D. (2002). Fluorescence resonance energy transfer analysis of protein-protein interactions in single living cells by multifocal multiphoton microscopy. J. Biotechnol. *82*, 267–277.
14. Elbashir, S.M., Harborth, J., Weber, K., and Tuschl, T. (2002). Analysis of gene function in somatic mammalian cells using small interfering RNAs. Methods *26*, 199–213.
15. Lin, R., Warn-Cramer, B.J., Kurata, W.E., and Lau, A.F. (2001). v-Src phosphorylation of connexin 43 on Tyr247 and Tyr265 disrupts gap junctional communication. J. Cell Biol. *154*, 815–827.
16. TenBroek, E.M., Lampe, P.D., Solan, J.L., Reynhout, J.K., and Johnson, R.G. (2001). Ser364 of connexin43 and the upregulation of gap junction assembly by cAMP. J. Cell Biol. *155*, 1307–1318.
17. Faucheux, N., Zahm, J.M., Bonnet, N., Legeay, G., and Nagel, M.D. (2004). Gap junction communication between cells aggregated on a cellulose-coated polystyrene: influence of connexin 43 phosphorylation. Biomaterials *25*, 2501–2506.
18. Ishikawa, R., Hayashi, K., Shirao, T., Xue, Y., Takagi, T., Sasaki, Y., and Kohama, K. (1994). Drebrin, a development-associated brain protein from rat embryo, causes the dissociation of tropomyosin from actin filaments. J. Biol. Chem. *269*, 29928–29933.
19. Shirao, T., and Sekino, Y. (2001). Clustering and anchoring mechanisms of molecular constituents of postsynaptic scaffolds in dendritic spines. Neurosci. Res. *40*, 1–7.
20. Takahashi, H., Sekino, Y., Tanaka, S., Mizui, T., Kishi, S., and Shirao, T. (2003). Drebrin-dependent actin clustering in dendritic filopodia governs synaptic targeting of postsynaptic density-95 and dendritic spine morphogenesis. J. Neurosci. *23*, 6586–6595.
21. Jamora, C., and Fuchs, E. (2002). Intercellular adhesion, signalling and the cytoskeleton. Nat. Cell Biol. *4*, E101–E108.
22. Yonemura, S., Itoh, M., Nagafuchi, A., and Tsukita, S. (1995). Cell-to-cell adherens junction formation and actin filament organization: similarities and differences between non-polarized fibroblasts and polarized epithelial cells. J. Cell Sci. *108*, 127–142.
23. Itoh, M., Nagafuchi, A., Moroi, S., and Tsukita, S. (1997). Involvement of ZO-1 in cadherin-based cell adhesion through its direct binding to alpha catenin and actin filaments. J. Cell Biol. *138*, 181–192.
24. Rajasekaran, A.K., Hojo, M., Huima, T., and Rodriguez Boulan, E. (1996). Catenins and zonula occludens-1 form a complex during early stages in the assembly of tight junctions. J. Cell Biol. *132*, 451–463.
25. Harigaya, Y., Shoji, M., Shirao, T., and Hirai, S. (1996). Disappearance of actin-binding protein, drebrin, from hippocampal synapses in Alzheimer's disease. J. Neurosci. Res. *43*, 87–92.
26. Nagy, J.I., Li, W., Hertzberg, E.L., and Marotta, C.A. (1996). Elevated connexin-43 immunoreactivity at sites of amyloid plaques in Alzheimer's disease. Brain Res. *717*, 173–178.
27. Westfall, T.A., Hjertos, B., Twedt, J., Brimeyer, R., Gladon, J., Olberding, A., Furutani-Seiki, M., and Slusarski, D.C. (2003). Wnt-5/pipetail functions in vertebrate axis formation as a negative regulator of Wnt/β-catenin activity. J. Cell Biol. *162*, 889–898.
28. Falk, M.M., Kumar, N.M., and Gilula, N.B. (1994). Membrane insertion of gap junction connexins: polytopic channel forming membrane proteins. J. Cell Biol. *127*, 343–354.
29. Toda, M., Shirao, T., Minoshima, S., Shimizu, N., Toya, S., and Uyemura, K. (1993). Molecular cloning of cDNA encoding human drebrin E and chromosomal mapping of its gene. Biochem. Biophys. Res. Commun. *196*, 468–472.
30. Tokuyasu, K.T. (1978). A study of positive staining of ultrathin frozen sections. J. Ultrastruct. Res. *63*, 287–307.
31. Allison, D.W., Chervin, A.S., Gelfand, V.I., and Craig, A.M. (2000). Postsynaptic scaffolds of excitatory and inhibitory synapses in hippocampal neurons: maintenance of core components independent of actin filaments and microtubules. J. Neurosci. *20*, 4545–4554.

Human Molecular Genetics Advance Access originally published online on November 24, 2004
Human Molecular Genetics 2005 14(2):241–253; doi:10.1093/hmg/ddi022

This Article

- Full Text
- Full Text (PDF)
- Supplementary Material
- All Versions of this Article: 14/2/241 *most recent* ddi022v1
- Alert me when this article is cited
- Alert me if a correction is posted

Services

- Email this article to a friend
- Similar articles in this journal
- Similar articles in PubMed
- Download to citation manager

PubMed

- PubMed Citation
- Articles by Iwamoto, K.
- Articles by Kato, T.

Altered expression of mitochondria-related genes in postmortem brains of patients with bipolar disorder or schizophrenia, as revealed by large-scale DNA microarray analysis

Kazuya Iwamoto, Miki Bundo and Tadafumi Kato*

Laboratory for Molecular Dynamics of Mental Disorders, Brain Science Institute, RIKEN, Wako, Saitama 351-0198, Japan

* To whom correspondence should be addressed at: Laboratory for Molecular Dynamics of Mental Disorders, Brain Science Institute, RIKEN, Hirosawa 2-1, Wako, Saitama 351-0198, Japan. Tel: +81 484676949; Fax: +81 484676947; Email: kato@brain.riken.go.jp

Received August 18, 2004; Revised October 15, 2004; Accepted November 9, 2004

Accumulating evidence suggests that mitochondrial dysfunction underlies the pathophysiology of bipolar disorder (BD) and schizophrenia (SZ). We performed large-scale DNA microarray analysis of postmortem brains of patients with BD or SZ, and examined expression patterns of mitochondria-related genes. We found a global down-regulation of mitochondrial genes, such as those encoding respiratory chain components, in BD and SZ samples, even after the effect of sample pH was controlled. However, this was likely due to the effects of medication. Medication-free patients with BD showed tendency of up-regulation of subset of mitochondrial genes. Our findings support the mitochondrial dysfunction hypothesis of BD and SZ pathologies. However, it may be the expression changes of a small fraction of mitochondrial genes rather than the global down-regulation of mitochondrial genes. Our findings warrant further study of the molecular mechanisms underlying mitochondrial dysfunction in BD and SZ.

Association of Mitochondrial Complex I Subunit Gene *NDUFV2* at 18p11 with Bipolar Disorder in Japanese and the National Institute of Mental Health Pedigrees

Shinsuke Washizuka, Kazuya Iwamoto, An-a Kazuno, Chihiro Kakiuchi, Kanako Mori, Mizue Kametani, Kazuo Yamada, Hiroshi Kunugi, Osamu Tajima, Tsuyoshi Akiyama, Shinichiro Nanko, Takeo Yoshikawa, and Tadafumi Kato

Background: *Linkage with 18p11 is one of the replicated findings in molecular genetics of bipolar disorder. Because mitochondrial dysfunction has been suggested in bipolar disorder,* NDUFV2 *at 18p11, encoding a subunit of the complex I, reduced nicotinamide adenine dinucleotide (NADH) ubiquinone oxidoreductase, is a candidate gene for this disorder. We previously reported that a polymorphism in the upstream region of* NDUFV2, *−602G> A, was associated with bipolar disorder in Japanese subjects; however, functional significance of −602G> A was not known.*

Methods: *We screened the further upstream region of* NDUFV2. *We performed a case–control study in Japanese patients with bipolar disorder and control subjects and a transmission disequilibrium test in 104 parent and proband trios of the National Institute of Mental Health (NIMH) Genetics Initiative pedigrees. We also performed the promoter assay to examine functional consequence of the −602G> A polymorphism.*

Results: *The −602G> A polymorphism was found to alter the promoter activity. We found that the other haplotype block surrounding −3542G> A was associated with bipolar disorder. The association of the haplotypes consisting of −602G> A and −3542G> A polymorphisms with bipolar disorder was seen both in Japanese case–control samples and NIMH trios.*

Conclusion: *Together these findings indicate that the polymorphisms in the promoter region of* NDUFV2 *are a genetic risk factor for bipolar disorder by affecting promoter activity.*

Key Words: Bipolar disorder, haplotype, mitochondria, NADH ubiquinone oxidoreductase, promoter assay, transmission disequilibrium test

The etiology of bipolar disorder (BD) is still unknown, but family, twin, and adoption studies strongly suggest the involvement of genetic risk factors (Goodwin and Jamison 1990). Linkage studies have revealed a number of loci to be linked with BD. Of those, several investigators confirmed 18p11 as one susceptibility loci for BD (Berrettini et al 1997; Gershon et al 1996; Nothen et al 1999; Stine et al 1995; Turecki et al 1999). Nominally significant linkage of BD with chromosome 18 was also found in a recent extensive meta-analysis (Segurado et al 2003). Thus, 18p is one of the targets of the genetic association study of BD.

We have proposed a mitochondrial dysfunction hypothesis of BD (Kato and Kato 2000) on the basis of the following evidence: altered brain energy metabolism in patients with BD detected by phosphorus-31 magnetic resonance spectroscopy (Kato et al 1993), increased ratio of the mitochondrial DNA (mtDNA) deletion in the brains of patients with BD (Kato et al 1997), association with mtDNA polymorphisms causing amino acid substitutions in the subunits of complex I (reduced nicotinamide adenine dinucleotide [NADH]: ubiquinone oxidoreductase; Kato et al 2001).

From the Laboratories for Molecular Dynamics of Mental Disorders (SW, KI, AK, CK, KM, MK, TK) and Molecular Psychiatry (KY, TY), Brain Science Institute, RIKEN, Wako, Saitama; Department of Mental Disorder Research (HK), National Institute of Neuroscience; Kyorin University School of Health Sciences (OT); Department of Neuropsychiatry (TA), NTT East Kanto Medical Center; and Department of Psychiatry and Genome Research Center (SN), Teikyo University School of Medicine, Tokyo, Japan.

Address reprint requests to Tadafumi Kato, M.D., Ph.D., Laboratory for Molecular Dynamics of Mental Disorders, Brain Science Institute, RIKEN, Hirosawa 2-1, Wako, Saitama, 351-0198, Japan; E-mail: kato@brain.riken.go.jp.

Received March 9, 2004; revised June 22, 2004; accepted July 5, 2004.

Complex I catalyzes the transfer of electrons from NADH to ubiquinone and the largest and most complicated enzyme in the mitochondrial electron transport chain, consisting of at least 43 subunits. Whereas seven subunits of complex I are coded in the mtDNA, the others are coded in the nuclear genome (Smeitink et al 2001). Of those, *NDUFV2* is located at 18p11 (de Coo et al 1995; Hattori et al 1995) and is a candidate gene for BD. Recently, Nakatani et al (2004) examined the gene expression patterns in the frontal cortex and hippocampus in animal models of depression and reported that *NDUFV2* was one of two genes altered in both regions. Moreover, Karry et al (2004) reported that protein levels of 24kDa subunit of complex I encoded by *NDUFV2* were altered in the autopsied brains of BD patients. These findings suggested a possible role of *NDUFV2* in mood disorders.

We previously screened mutations and polymorphisms in all exons and the 1-kb upstream region of *NDUFV2* in BD patients and reported that a polymorphism, −602G> A, in the upstream region was significantly associated with BD in Japanese (Washizuka et al 2003). The mRNA expression of *NDUFV2* was also significantly decreased in the lymphoblastoid cells of patients with bipolar I disorder.

In this study, we further screened the 4kb-upstream region of the *NDUFV2* and examined the association with BD in a Japanese case–control samples. Furthermore, we performed a promoter assay to examine the functional significance of the −602G> A polymorphism, which determines the major haplotypes associated with BD. We then examined whether a similar association was found in the National Institute of Mental Health (NIMH) Initiative Genetics Bipolar Pedigrees by the haplotype transmission disequilibrium test (TDT).

Methods and Materials

Japanese Case–Control Samples

The subjects with BD were 189 unrelated patients (117 women and 72 men, 136 with bipolar I disorder (BDI) and 53

0006-3223/04/$30.00
doi:10.1016/j.biopsych.2004.07.004